their transcription is completely silent in normal cells, an RT-PCR-based detection kit would be of practical value. The genes in Tables 2 and 3 are our first results from the approaches above, and expression profiles of some of them were confirmed by real-time PCR (Fig. 3).

Among the genes listed in Tables 2 and 3, several were already known to be highly expressed in carcinoma cells. For example, ID2 drives cell cycle progression by interacting with, and suppressing the activity of, a tumor suppressor, Rb.[23] ID2 can also suppress another growth suppressor, p16.

CEACAM7 belongs to the CEA family of proteins. In contrast to the high level of expression of CEA apparent in colorectal carcinomas, CEACAM7 is abundant in normal colonic epithelium and its expression is down-regulated during malignant transformation.[24,25] Although its expression in pancreas has not been well characterized, previous data indicate that CEACAM7 is expressed in normal pancreatic ductal cells.[24] However, our observation that the *CEACAM7* gene is preferentially expressed in ductal cells of PDC patients suggests that this gene is a potential marker for cancer diagnosis with either ductal cell- or serum-based assays.

AC133 was initially identified as a cell surface marker specific to a hematopoietic stem cell-enriched fraction with a $CD34^{high}$, $CD38^{low}$ or $CD38^{-}$, and c-Kit^{+} phenotype.[26] This protein is also expressed on the precursor of endothelial cells,[27] indicating that it may be a marker for immature hemangioblasts, which are common precursors for blood cells and blood vessels. Although expression of AC133 in tissues other than bone marrow and the retina has not been previously demonstrated, we have now shown that the *AC133* gene is expressed in the pancreatic ductal cells of PDC patients. Given the abundance of AC133 in normal hemangioblasts, the expression of the *AC133* gene in carcinoma ductal cells may suggest that AC133 is also a marker of the precursor for ductal cells. The increased expression of the *AC133* gene in PDC may thus reflect the immature nature of the cancer cells with regard to the differentiation program of ductal cells.

It should be noted, however, that none of the single genes listed in Tables 2 and 3 was able to distinguish all PDC samples from normal ductal cells. In addition to such single gene-based prediction systems, it may be possible to use the expression profiles of a combination of "class predictor" genes[28] for PDC diagnosis. We have indeed examined the feasibility of this approach with the statistically "disease-dependent" genes listed in Table 2. Prediction of PDC diagnosis was tried with the k-nearest neighbor algorithm by using the GeneSpring software (http://www.silicongenetics.com/Support/GeneSpring/GSnotes/class_prediction.pdf). In a "cross-validation" trial, all three ND samples were correctly diagnosed by the expression profiles of the disease-dependent genes (data not shown). With regard to the CD samples, four out of six samples were correctly predicted, and the other two were called "unpredictable." Therefore, among the nine ductal cell specimens, seven (77.8%) were correctly diagnosed. Selection of stronger "predictor" genes through large-scale microarray studies may make it possible to construct reliable "PDC diagnosis arrays" harboring a small number of such predictor genes.

In conclusion, we have shown that DNA microarray analysis with purified ductal cell fractions is a promising approach to the identification of PDC-specific genes, being greatly superior to a mere comparison of tissue specimens. Our data thus provide a basis for the possible development of an ERCP-dependent sensitive and specific test for the detection of pancreatic cancer.

This work was supported in part by a Grant-in-Aid for Scientific Research (C) from the Ministry of Education, Culture, Sports, Science and Technology, Japan.

1. Bornman PC, Beckingham IJ. Pancreatic tumours. *Br Med J* 2001; 322: 721–3.
2. Rosewicz S, Wiedenmann B. Pancreatic carcinoma. *Lancet* 1997; 349: 485–9.
3. Adamek HE, Albert J, Breer H, Weitz M, Schilling D, Riemann JF. Pancreatic cancer detection with magnetic resonance cholangiopancreatography and endoscopic retrograde cholangiopancreatography: a prospective controlled study. *Lancet* 2000; 356: 190–3.
4. Kondo H, Sugano K, Fukayama N, Kyogoku A, Nose H, Shimada K, Ohkura H, Ohtsu A, Yoshida S, Shimosato Y. Detection of point mutations in the K-ras oncogene at codon 12 in pure pancreatic juice for diagnosis of pancreatic carcinoma. *Cancer* 1994; 73: 1589–94.
5. Sugano K, Nakashima Y, Yamaguchi K, Fukayama N, Maekawa M, Ohkura H, Kakizoe T, Sekiya T. Sensitive detection of loss of heterozygosity in the TP53 gene in pancreatic adenocarcinoma by fluorescence-based single-strand conformation polymorphism analysis using blunt-end DNA fragments. *Genes Chromosom Cancer* 1996; 15: 157–64.
6. Caldas C, Hahn SA, da Costa LT, Redston MS, Schutte M, Seymour AB, Weinstein CL, Hruban RH, Yeo CJ, Kern SE. Frequent somatic mutations and homozygous deletions of the p16 (MTS1) gene in pancreatic adenocarcinoma. *Nat Genet* 1994; 8: 27–32.
7. Hahn SA, Schutte M, Hoque AT, Moskaluk CA, da Costa LT, Rozenblum E, Weinstein CL, Fischer A, Yeo CJ, Hruban RH, Kern SE. DPC4, a candidate tumor suppressor gene at human chromosome 18q21.1. *Science* 1996; 271: 350–3.
8. Hohne MW, Halatsch ME, Kahl GF, Weinel RJ. Frequent loss of expression of the potential tumor suppressor gene DCC in ductal pancreatic adenocarcinoma. *Cancer Res* 1992; 52: 2616–9.
9. Furuya N, Kawa S, Akamatsu T, Furihata K. Long-term follow-up of patients with chronic pancreatitis and K-ras gene mutation detected in pancreatic juice. *Gastroenterology* 1997; 113: 593–8.
10. Duggan DJ, Bittner M, Chen Y, Meltzer P, Trent JM. Expression profiling using cDNA microarrays. *Nat Genet* 1999; 21: 10–4.
11. Schena M, Shalon D, Davis RW, Brown PO. Quantitative monitoring of gene expression patterns with a complementary DNA microarray. *Science* 1995; 270: 467–70.
12. Miyazato A, Ueno S, Ohmine K, Ueda M, Yoshida K, Yamashita Y, Kaneko T, Mori M, Kirito K, Toshima M, Nakamura Y, Saito K, Kano Y, Furusawa S, Ozawa K, Mano H. Identification of myelodysplastic syndrome-specific genes by DNA microarray analysis with purified hematopoietic stem cell fraction. *Blood* 2001; 98: 422–7.
13. Van Gelder RN, von Zastrow ME, Yool A, Dement WC, Barchas JD, Eberwine JH. Amplified RNA synthesized from limited quantities of heterogeneous cDNA. *Proc Natl Acad Sci USA* 1990; 87: 1663–7.
14. Balague C, Audie JP, Porchet N, Real FX. *In situ* hybridization shows distinct patterns of mucin gene expression in normal, benign, and malignant pancreas tissues. *Gastroenterology* 1995; 109: 953–64.
15. Terada T, Ohta T, Sasaki M, Nakamura Y, Kim YS. Expression of MUC apomucins in normal pancreas and pancreatic tumours. *J Pathol* 1996; 180: 160–5.
16. Lacobuzio-Donahue CA, Maitra A, Shen-Ong GL, van Heek T, Ashfaq R, Meyer R, Walter K, Berg K, Hooingsworth MA, Cameron JL, Yeo CJ, Kern SE, Goggins M, Hruban RH. Discovery of novel tumor markers of pancreatic cancer using global gene expression technology. *Am J Pathol* 2002; 160: 1239–49.
17. Alon U, Barkai N, Notterman DA, Gish K, Ybarra S, Mack D, Levine AJ. Broad patterns of gene expression revealed by clustering analysis of tumor and normal colon tissues probed by oligonucleotide arrays. *Proc Natl Acad Sci USA* 1999; 96: 6745–50.
18. Hay RT. Protein modification by SUMO. *Trends Biochem Sci* 2001; 26: 332–3.
19. Johnson ES, Gupta AA. An E3-like factor that promotes SUMO conjugation to the yeast septins. *Cell* 2001; 106: 735–44.
20. Luo L, Salunga RC, Guo H, Bittner A, Joy KC, Galindo JE, Xiao H, Rogers KE, Wan JS, Jackson MR, Erlander MG. Gene expression profiles of laser-captured adjacent neuronal subtypes. *Nat Med* 1999; 5: 117–22.
21. Ho SB, Niehans GA, Lyftogt C, Yan PS, Cherwitz DL, Gum ET, Dahiya R, Kim YS. Heterogeneity of mucin gene expression in normal and neoplastic tissues. *Cancer Res* 1993; 53: 641–51.
22. Osako M, Yonezawa S, Siddiki B, Huang J, Ho JJL, Kim YS, Sato E. Immunohistochemical study of mucin carbohydrates and core proteins in human pancreatic tumors. *Cancer* 1993; 71: 2191–9.
23. Lavarone A, Garg P, Lasorella A, Hsu J, Israel MA. The helix-loop-helix protein Id-2 enhances cell proliferation and binds to the retinoblastoma protein. *Genes Dev* 1994; 8: 1270–84.
24. Scholzel S, Zimmermann W, Schwarzkopf G, Grunert F, Rogaczewski B, Thompson J. Carcinoembryonic antigen family members CEACAM6 and

CEACAM7 are differentially expressed in normal tissues and oppositely deregulated in hyperplastic colorectal polyps and early adenomas. *Am J Pathol* 2000; 156: 595–605.
25. Thompson J, Seitz M, Chastre E, Ditter M, Aldrian C, Gespach C, Zimmermann W. Down-regulation of carcinoembryonic antigen family member 2 expression is an early event in colorectal tumorigenesis. *Cancer Res* 1997; 57: 1776–84.
26. Hin AH, Miraglia S, Zanjani ED, Almeida-Porada G, Ogawa M, Leary AG, Olweus J, Kearney J, Buck DW. AC133, a novel marker for human hematopoietic stem and progenitor cells. *Blood* 1997; 90: 5002–12.
27. Gallacher L, Murdoch B, Wu DM, Karanu FN, Keeney M, Bhatia M. Isolation and characterization of human CD34(−)Lin(−) and CD34(+)Lin(−) hematopoietic stem cells using cell surface markers AC133 and CD7. *Blood* 2000; 95: 2813–20.
28. Golub TR, Slonim DK, Tamayo P, Huard C, Gaasenbeek M, Mesirov JP, Coller H, Loh ML, Downing JR, Caligiuri MA, Bloomfield CD, Lander ES. Molecular classification of cancer: class discovery and class prediction by gene expression monitoring. *Science* 1999; 286: 531–7.

Available online at www.sciencedirect.com
SCIENCE DIRECT®
Biochemical and Biophysical Research Communications 307 (2003) 771–777
BBRC
www.elsevier.com/locate/ybbrc

DNA microarray analysis of in vivo progression mechanism of heart failure☆

Shuichi Ueno,[a,b] Ruri Ohki,[a,b] Toru Hashimoto,[a,b] Toshihiro Takizawa,[c] Koichi Takeuchi,[c] Yoshihiro Yamashita,[a] Jun Ota,[a,d] Young Lim Choi,[a] Tomoaki Wada,[a] Koji Koinuma,[a] Keiji Yamamoto,[b] Uichi Ikeda,[b] Kazuyuki Shimada,[b] and Hiroyuki Mano[a,d,*]

[a] *Division of Functional Genomics, Jichi Medical School, 3311-1 Yakushiji, Kawachi-gun, Tochigi 329-0498, Japan*
[b] *Division of Cardiology, Jichi Medical School, 3311-1 Yakushiji, Kawachi-gun, Tochigi 329-0498, Japan*
[c] *Department of Anatomy, Jichi Medical School, 3311-1 Yakushiji, Kawachi-gun, Tochigi 329-0498, Japan*
[d] *CREST, JST, Saitama 332-0012, Japan*

Received 11 June 2003

Abstract

Dahl salt-sensitive rats are genetically hypersensitive to sodium intake. When fed a high sodium diet, they develop systemic hypertension, followed by cardiac hypertrophy and finally heart failure within a few months. Therefore, Dahl rats represent a good model with which to study how heart failure is developed in vivo. By using DNA microarray, we here monitored the transcriptome of >8000 genes in the left ventricular muscles of Dahl rats during the course of cardiovascular damage. Expression of the atrial natriuretic peptide gene was, for instance, induced in myocytes by sodium overload and further enhanced even at the heart failure stage. Interestingly, expression of the gene for the D-binding protein, an apoptotic-related transcriptional factor, became decreased upon the transition to heart failure. To our best knowledge, this is the first report to describe the transcriptome of cardiac myocytes during the disease progression of heart failure.

Keywords: DNA microarray; Dahl salt-sensitive rat; DBP; Heart failure; Hypertension

A variety of conditions including pressure or volume overload lead to hypertrophy of cardiac muscles, which is often accompanied with an increase in systemic blood pressure (BP). The hypertrophic change is in some cases the result of a compensatory mechanism and in other cases due to yet unidentified causes. Regardless of the etiology, however, sustained hypertrophy of cardiac myocytes eventually induces a reduction in contractile ability and/or a decrease in the number of viable myocytes; the condition referred to as "heart failure" [1]. Even today, it is difficult to control the function of failed heart and this condition remains one of the leading causes of human death [2]. The possibility of preventing the progression from cardiac hypertrophy to heart failure would be greatly increased by characterization of this process at the molecular level.

Unfortunately, however, little information has been provided on this issue. Studies with neonatal rat cardiac myocytes cultured in vitro, for example, have provided important insight into the mechanism by which these cells become hypertrophic in response to various conditions [3]. However, the clarification of the next step, transition to pumping failure, should require the analysis of in vivo specimens from both hypertrophic and failed hearts. Sampling of ventricle myocytes from human patients is very difficult, especially in a large scale or in a time-course manner.

☆ *Abbreviations:* BP, blood pressure; LV, left ventricular; EF, ejection fraction; RT, reverse transcription; PCR, polymerase chain reaction; ANP, atrial natriuretic peptide; PAP, pancreatitis-associated protein; DBP, D-binding protein; ET, endothelin; AT, angiotensin.

* Corresponding author. Fax: +81-285-44-7322.
E-mail address: hmano@jichi.ac.jp (H. Mano).

0006-291X/03/$ - see front matter © 2003 Elsevier Inc. All rights reserved.
doi:10.1016/S0006-291X(03)01252-X

To circumvent this hurdle, appropriate model animals would be required, in which hypertension–hypertrophy and heart failure is induced in this order, either naturally or by some treatments. Dahl et al. isolated a mutant strain from Sprague–Dawley rats, which exhibits a genetical hypersensitivity to sodium intake [4]. With a high sodium diet, this "Dahl salt-sensitive" rat developed systemic hypertension and cardiac hypertrophy within a few weeks. Importantly, these changes were followed by the development of congestive heart failure and death in a few months. Therefore, by using the Dahl rats, we could observe how hypertrophy of heart is transformed in vivo into congestive failure.

DNA microarray has revolutionized our way to analyze the gene expression profile. It enables us to monitor the expression level of thousands of genes simultaneously and provides us the "transcriptome" profiles of given cells or tissues [5]. Therefore, DNA microarray would be one of the most suitable approaches to address the gene expression alterations that account for the progression of heart failure. In this paper, we fed Dahl salt-sensitive rats high- or low-sodium diet and compared the transcriptomes of cardiac myocytes at various stages in the affected and control rats. We thereby identified various groups of genes whose expression is dependent on the stage of heart disease.

Materials and methods

Preparation of cardiac myocytes from Dahl salt-sensitive rats. Dahl salt-sensitive rats ($n = 36$) were obtained from Japan SLC (Shizuoka, Japan). They were fed a low-sodium diet (containing 0.3% NaCl) until the age of 6 weeks. Sixteen rats were then switched to a high-sodium diet (containing 8% NaCl), whereas the remaining 20 animals were maintained on the low-sodium diet. Both groups of rats were monitored every week for BP, body weight (BW), thickness of left ventricular (LV) posterobasal free wall, and LV ejection fraction (EF). The latter two were measured by echocardiography (7.5-MHz transducer; Sonos 2000, Hewlett-Packard, Andover, MA) after anesthesia with an intramuscular injection of pentobarbital sodium (15 mg/kg BW). Four rats from each group were killed at ages of 6, 8, 11, 13, and 15 weeks; two of the animals were subjected to pathological examination and the other two were used as a source of LV muscle for DNA microarray analysis.

RNA preparation and DNA microarray analysis. Total RNA was extracted from the LV specimens with the use of RNAzol B (Tel-Test, Friendswood, TX), and a portion (20 μg) was converted to double-stranded cDNA by the SuperScript Choice System (Life Technologies, Gaithersburg, MD) with the T7–dT primer (5′-TCTAGTCGA CGGCCAGTGAATTGTAATACGACTCACTATAGGGCGTTTT TTTTTTTTTTTTTTTT-3′). Biotin-labeled cRNA was prepared from the resulting cDNA with the use of ENZO BioArray RNA labeling kit (ENZO Diagnostics, Farmingdale, NY) and hybridized with the GeneChip Rat U34A array (Affymetrix, Santa Clara, CA) harboring the oligonucleotides corresponding to 8799 genes. Washing of the arrays and detection of the hybridized cRNAs were performed with the GeneChip instrument system according to the manufacturer's protocol.

The fluorescence intensity of each gene was normalized relative to the median fluorescence value for all genes in each chip hybridization. Statistical analysis of the digitized data was performed with GeneSpring 4.0 software (Silicon Genetics, Redwood, CA).

All array data as well as the information for the genes shown in Fig. 3 are available through the web site of *Biochem. Biophys. Res. Commun.*

"Real-time" reverse transcription-polymerase chain reaction (RT-PCR) analysis. Portions of the double-stranded cDNAs were subjected to PCR with SYBR Green PCR Core Reagents (PE Applied Biosystems, Foster City, CA). Incorporation of the SYBR Green dye into the PCR products was monitored in real time with an ABI PRISM 7700 sequence detection system (PE Applied Biosystems), resulting in the calculation of threshold cycle, or C_T value, that defines the PCR cycle number at which an exponential growth of PCR products begins. The C_T values for glyceraldehyde-3-phosphate dehydrogenase (GAPDH) gene and for genes of interest were used to calculate the abundance of the transcripts of these latter genes relative to that of GAPDH mRNA. The oligonucleotide primers for PCR were 5′-ACCACAGTCCAT GCCATCAC-3′ and 5′-TCCACCACCCTGTTGCTGTA-3′ for GAPDH cDNA, 5′-GGTAGGATTGACAGGATTGGAGCC-3′ and 5′-ACATCGATCGTGATAGATGAAGAC-3′ for atrial natriuretic peptide (ANP) cDNA, 5′-TATACCTGGATTGGACTCCATGAC-3′ and 5′-CTTGACAGGATGTGCTTCAGGACA-3′ for pancreatitis-associated protein (PAP) cDNA, 5′-CATCACCATGTGCATCTTC ACGTG-3′ and 5′-AGGAGCCAAACGACATTTATCTGG-3′ for 12-lipoxygenase cDNA, and 5′-GCCTCAGCCAATCATGAAGAAG GC-3′ and 5′-TAGCGTGAAAGCACAGCACGGTAG-3′ for D-binding protein (DBP) cDNA. Amplification of the target products with these primers was verified prior to the real-time PCR analysis.

Results

Development of cardiac hypertrophy and heart failure in Dahl salt-sensitive rats

Dahl salt-sensitive rats were fed either a high- or low-sodium diet and their cardiovascular parameters were monitored. The initial systolic BP at 6 weeks of age was 108.5 ± 11.4 mmHg (mean ± SD, $n = 36$). Animals on the high-sodium diet, however, exhibited a rapid increase in BP to 163.8 ± 9.2 and 227.1 ± 19.6 mmHg after 2 and 4 weeks, respectively, whereas the systolic BP of rats maintained on the low-sodium diet remained within the normal range (121.9 ± 4.3 mmHg after 4 weeks) (Fig. 1A).

In parallel with the progression of systemic hypertension, LV wall thickness also rapidly increased with sodium loading (Fig. 1B). Within 2 weeks of high sodium intake, LV weight per tibial bone length (LVW/TL) changed from 118.12 ± 5.0 to 203.9 ± 9.3 mg/cm, while that of the low-sodium group slowly increased to 142.2 ± 4.9 mg/cm during this time interval.

Although the development of systemic hypertension and cardiac hypertrophy was rapid and almost simultaneous, the pumping function of hearts in the high-sodium group remained normal up to 11 weeks of age (Fig. 1C). Thereafter, however, the LV EF of these animals became rapidly impaired; $85.6 \pm 2.1\%$, $71.1 \pm 3.5\%$, and $61.0 \pm 1.0\%$ at 11, 13, and 15 weeks of age, respectively. In contrast, the EF of rats in the low-sodium group remained at a high level ($87.0 \pm 0.9\%$ at

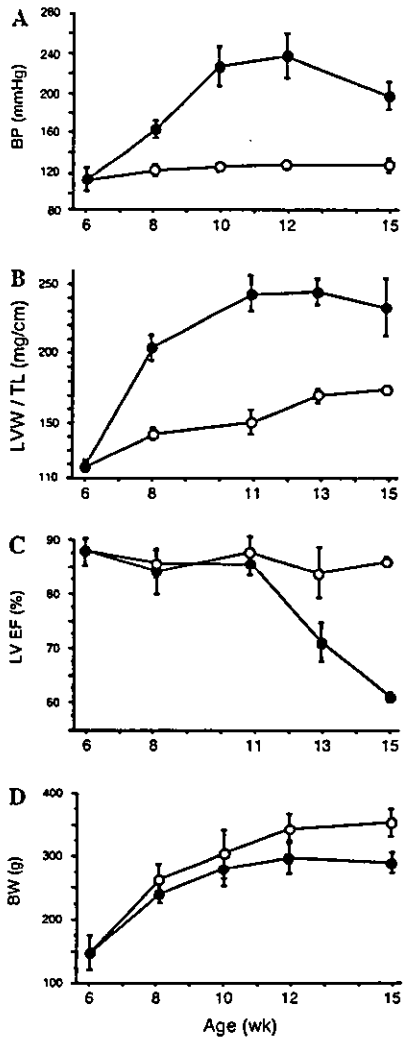

Fig. 1. Disease progression in Dahl salt-sensitive rats. Changes in systolic BP (A), LVW/TL (B), LV EF (C), and BW (D) in Dahl salt-sensitive rats fed a diet containing 8% NaCl (closed circle) or 0.3% NaCl (open circle) from the age of 6 weeks are shown as mean values ± SD ($n = 4$ to 36).

15 weeks of age). The appetite of rats decreased upon the onset of heart failure and the previous steady increase in BW ceased at this stage (Fig. 1D). Most of the animals with the high-sodium intake died between 15 and 18 weeks of age.

It should be noted that pumping failure developed after a certain interval of hypertrophic stage, which resembles well the clinical course in human heart diseases. Patients with a high BP maintain a high LV EF at an early stage of disease; many of them, however, eventually undergo heat failure despite clinical treatment. Therefore, investigation of the transition process from cardiac hypertrophy to heart failure in Dahl salt-sensitive rats may provide us clues to the molecular events essential for the progression to heart failure.

Pathological examination of the Dahl salt-sensitive rats also supported our hypothesis that those with the high-sodium diet well follow the natural course of heart failure in humans. In contrast to the LV myocytes of rats at 6 weeks of age, those from animals subjected to sodium overload for 2 weeks (8 weeks old) exhibited marked hypertrophy (Figs. 2A and B). Furthermore, cross-sections of the sodium-loaded rats at 15 weeks of age clearly demonstrated the feature characteristic to the failed heart in humans; a decrease in the number of viable myocytes, an increase in the amount of fibrotic tissue, and lymphocyte infiltration (Fig. 2C). None of these changes associated with hypertrophy or heart failure were observed in the specimens from the rats with low-sodium intake (data not shown).

Genes induced with the development of hypertension/hypertrophy

LV tissue samples were prepared from two rats at 6 weeks old (normal stage), and from the ones with the high-sodium diet at 8 weeks old (early hypertension stage), 11 weeks old (late hypertension stage), 13 weeks old (early heart failure stage), and 15 weeks old (late heart failure stage). The samples were also obtained from the age-matched controls with the low-sodium diet and all of them were subjected to DNA microarray analysis. The mean expression level for each gene calculated from the GeneChip data of the two rats was used for statistical analysis.

To visualize the expression levels of the >8000 genes in LV cells at each stage, we here generated a dendrogram, or "gene tree," in which genes of similar expression pattern during the disease progression are placed nearby. The extent of such similarity was measured by the standard correlation with a separation ratio of 0.5 (Fig. 3A). From this tree, it is apparent that the transcriptomes of LV cells from 6-, 8-, and 11-week-old rats fed the low-sodium diet are similar to each other. Statistical "two-way clustering" [6] of the samples also grouped these three samples within the same branch (data not shown). In contrast, observed in this figure were a number of gene clusters that were induced in the rats with sodium overload at 8 weeks or 11 weeks of age.

A total of four genes (seven independent spot-groups on the array) were identified by the extraction of genes whose expression is highly induced in sodium-loaded rats at 8 weeks of age (early hypertrophic stage) compared with that in the age-matched controls (Fig. 3B). It may be notable that these genes can be separated into two sub-groups; one containing only the gene for ANP and the other containing the genes for β-actin, myosin heavy chain polypeptide 7, and aldolase A. While the gene for ANP was induced throughout the entire course, expression of the genes in the latter group decreased lately (at 13 or 15 weeks of age).

We next tried to isolate a group of genes whose expression level in the sodium-loaded rats at 11 weeks of

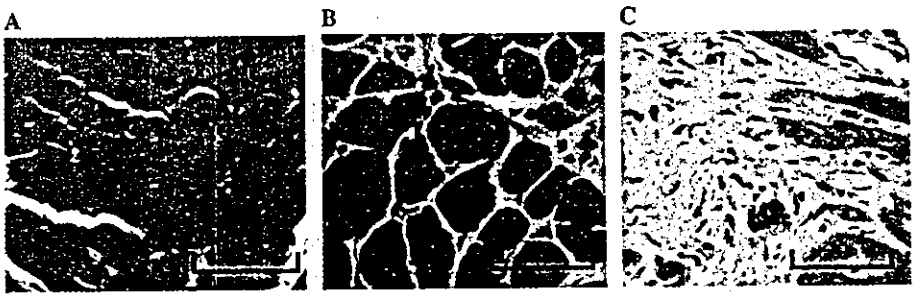

Fig. 2. Pathological examination of LV specimens at normal, hypertrophic, and failing stages of heart disease. Dahl salt-sensitive rats at the normal stage (6 weeks old) (A), hypertrophic stage (8 weeks old) (B), and heart failure stage (15 weeks old) (C) were sacrificed, and the cross-sections of their left ventricles were stained with hematoxylin and eosin. Scale bars, 50 μm.

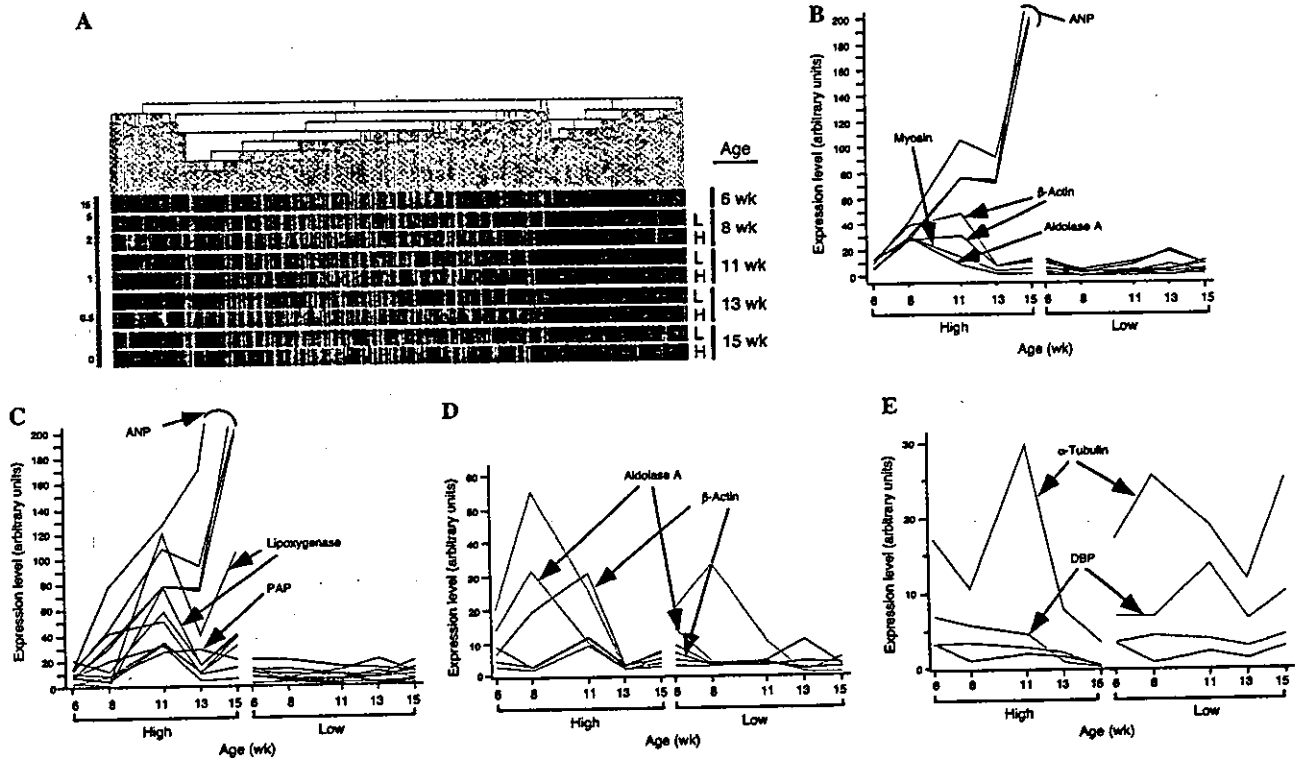

Fig. 3. Identification of genes expressed in a disease stage-specific manner. (A) Expression profiles of >8000 rat genes are shown as a dendrogram in which genes with similar expression pattern across the samples are positioned close to each other. RNA used for the analysis was obtained from rats of the indicated ages that were fed a diet low (L) or high (H) in sodium from 6 weeks of age. The fluorescence intensity of each gene was normalized relative to the mean value for all genes in each hybridization and is shown pseudocolored according to the scale on the left. (B) Expression profiles throughout the observation period for genes whose expression level at 8 weeks of age was markedly increased in rats fed the high-sodium diet (High) compared with that in animals fed the low-sodium diet (Low). Each curve corresponds to a single gene on the GeneChip and is color-coded according to the expression level at 8 weeks of age. Curves corresponding to the genes for ANP, myosin heavy chain polypeptide 7 (Myosin), β-actin, and aldolase A are indicated by arrows. (C) Expression profiles of genes whose expression level at 11 weeks of age was markedly increased in sodium-loaded rats compared with that in control animals. The curves are color-coded according to the expression level at 11 weeks of age. Curves corresponding to the genes for ANP, 12-lipoxygenase, and PAP are indicated. (D) Expression profiles of genes whose expression level increased at the hypertrophic stage (8–11 weeks of age) and decreased thereafter in the rats fed the high-sodium diet. The curves are color-coded according to the expression level at 13 weeks of age. Curves corresponding to the genes for aldolase A and β-actin are indicated. (E) Expression profiles of genes whose expression level decreased with the onset of heart failure in rats fed the high-sodium diet. The curves are color-coded according to the expression level in the sodium-loaded rats at 15 weeks of age. Curves corresponding to the genes for α-tubulin and DBP are indicated. The gene names and accession numbers as well as the expression intensity data for the genes shown in (B)–(E) are available through the web site of Biochem. Biophys. Res. Commun.

age (late hypertrophic stage) was highly induced compared to that in the age-matched controls. Seven genes (12 independent spot-groups on the array) were thus isolated (Fig. 3C). In addition to the four genes extracted above, the newly identified genes included those for PAP and 12-lipoxygenase.

Genes down-regulated along with the reduction in EF

Which genes are activated or down-regulated specifically in the heart failure stage? Our effort to isolate genes whose expression is only induced at this stage has resulted in failure. Therefore, we next focused on genes, expression of which was down-regulated in parallel with the reduction in EF.

For this purpose we attempted to extract genes with two distinct expression patterns. In one group, the genes were silent or expressed at a low level at the normal stage, became activated at the hypertrophic stage, but whose expression subsequently decreased at the heart failure stage. In the next group, the genes were active throughout the normal and hypertrophic stages, but became inactivated at the onset of heart failure (13 weeks of age).

We identified six genes whose expression profiles conformed to the first of these two patterns. The expression of all six genes was thus markedly down-regulated between 11 and 13 weeks of age in rats fed the high-salt diet (Fig. 3D). The expression of, for example, the β-actin gene was elevated throughout the hypertrophic stage (8–11 weeks of age), but became negligible once pumping failure began. The aldolase A gene showed a similar expression profile. Interestingly, neither of them was highly expressed in the rats on the low-sodium diet. Therefore, the expression level of these genes may reflect the contractile ability of LV muscles.

We identified four genes, including those for α-tubulin and DBP, whose expression profiles conformed to the second pattern (Fig. 3E). In contrast to the other two genes in this group, α-tubulin and DBP expressions were active throughout the normal and hypertrophic stages in both sodium-loaded and control rats, but declined only in the sodium-loaded group at the heart failure stage. In other words, the expression level of the two genes changed approximately in a parallel manner to the EF level.

Confirmation of expression level by real-time RT-PCR

We then quantified the mRNA level of the above genes by another method, real-time PCR. The abundance of ANP, 12-lipoxygenase, PAP, and DBP genes was determined relative to that of GAPDH mRNA in the LV specimens obtained from the rats with high- or low-sodium diet. Consistent with the results obtained by microarray analysis, the expression of ANP was kept increased throughout the study only in the sodium-loaded rats (Fig. 4A). Similarly, the real-time PCR confirmed the expression data for the other genes with the GeneChip system. The genes for 12-lipoxygenase (Fig. 4B) and PAP (Fig. 4C) started to increase at 11 weeks of age in the rats with high-sodium diet, but not with the low-sodium one. As shown in Fig. 4D, the expression of DBP was down-regulated along with the progression of heart failure, while it remained at a high

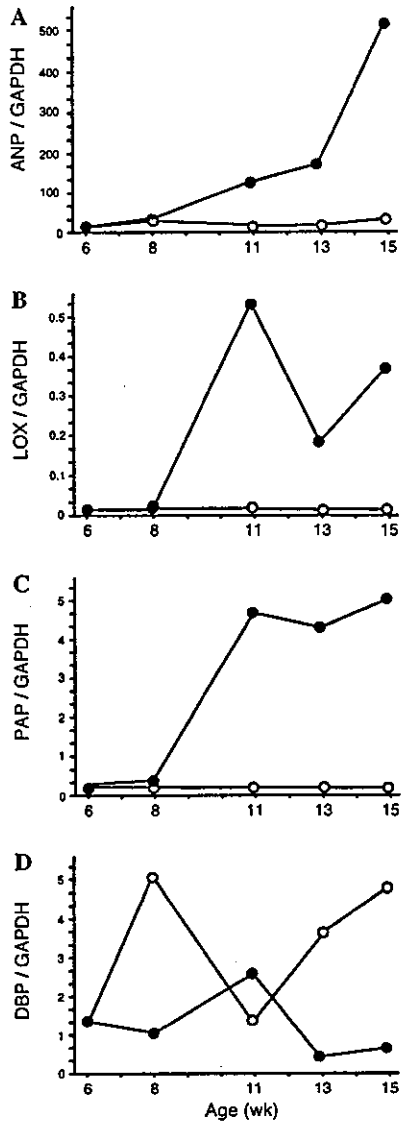

Fig. 4. Quantification of mRNA level by real-time PCR method. The cDNA prepared from LV tissue of Dahl salt-sensitive rats at the indicated ages after being fed a diet containing 8% NaCl (closed circles) or 0.3% NaCl (open circles) was subjected to real-time PCR analysis with primers specific for ANP (A), 12-lipoxygenase (LOX) (B), PAP (C), DBP (D), or GAPDH genes. The ratio of the abundance of the target transcripts to that of GAPDH mRNA was calculated as 2^n, where n is the C_T value for GAPDH cDNA minus the C_T value of the target cDNA.

level during the corresponding period in the rats with low-sodium diet (the reason for the transient decrease in the amount of this mRNA at 11 weeks of age in the control rats is not clear). Thus, overall, the results of the GeneChip analysis correlated well to those obtained by real-time RT-PCR method.

Discussion

In this paper, we have investigated the changes in expression level of a large number of genes in heart

muscles during the disease progression from normal state to cardiac hypertrophy, and subsequently to heart failure in Dahl salt-sensitive rats.

Although the genetic mutation(s) responsible for the salt-sensitivity of these animals remains to be identified, renal cross-transplantation experiment indicated that the primary defect to cause hypertension in the rats should reside within kidney [7]. Actually, feeding the rats a high-sodium diet induces marked changes in kidney morphology, leading to renal dysfunction [8]. Various studies have also implicated the renin–angiotensin (AT) system [9], calcinurin [10,11], endothelin (ET)-system [9,12], and interleukin (IL)-1β [13] in the development of LV hypertrophy and/or heart failure in Dahl salt-sensitive rats.

However, in the present screening, no significant difference was found between the rat LV muscles with the high-sodium and low-sodium intake for the expression levels of AT receptor genes, calcinurin-related genes, ET-related genes, and IL-1β, at least, for the genes included on the GeneChip U34A array (data not shown). Although our data do not exclude the possibility that any of the factors above are involved in the process of hypertrophy or pumping failure, these observations open the possibility of another primary cause which is turned on only in the sodium-overloaded state and evokes the catastrophe of cardiac function.

We could isolate many groups of genes whose expression behavior is highly dependent on the amount of sodium in the diet. For instance, expression of the ANP gene differed most markedly between the sodium-loaded and control rats; its expression was kept increased to the final stage in the rats fed the high-sodium diet, but remained negligible in the rats on the low-sodium one (Figs. 3B and C). ANP is a vasodilator released from atrium in response to pressure overload, but was also shown to be expressed in ventricle [14]. The pronounced increase in ANP gene expression observed in the present study may therefore result from the systemic hypertension and congestive heart failure that developed in sodium-loaded rats.

The increase in β-actin and myosin heavy chain gene expression observed during the development of hypertrophy likely reflects the associated increase in cardiac muscle mass and contractile ability. Consistent with this notion, the expression of both of these genes subsequently decreased with the progression to heart failure (Fig. 3B). It would also be possible that the increase of aldolase A gene is considered in the same context. Aldolase A is a ubiquitous protein and functions in the glycolysis process. Therefore, induction of aldolase A may reflect the elevated catabolic activity in the hypertrophic muscles. Diminution of its expression in the failure stage is compatible with this hypothesis.

The 12-lipoxygenase protein catalyzes the transfer of oxygen to the C-12 position of arachidonic acid. Although its in vivo function is not clear yet, it is of interest that the products of this enzyme may have a growth promoting activity [15,16]. The gene expression of 12-lipoxygenase is, at least partially, under the control of angiotensin II stimulation, and the metabolite of this enzyme can induce hypertrophy of vascular smooth muscle cells. Furthermore, Gabel et al. [17] indicated the cardioprotective effect of 12-lipoxygenase. Thus, overexpression of this gene only in the sodium-loaded rats may contribute to the development of hypertrophy, and the transient inactivation of the gene at the age of 13 weeks (Figs. 3C and 4B) may be related to the transition to the heart failure state.

PAP, also known as HIP [18], is known to be released from pancreas upon pancreatitis [19] and is related to C-type lectins. Based on its structural motifs, PAP is supposed to be involved in the cell-to-cell contact or cell migration, while its specific role in vivo is totally unknown. Functional role of sustained expression of PAP only in the rats with the high-sodium diet also remains to be elucidated.

From this study, the gene of potential interest may be that for DBP which belongs to the basic region-leucine zipper (bZIP) family of transcriptional factors [20]. Close relatives to DBP include thyrotroph embryonic factor (TEF) [21], hepatic leukemia factor (HLF) [22], and NFIL3/E4BP4 [23]. These proteins are likely to play a pivotal role in the determination of cell fate for apoptosis [24], and, thus, it was an interesting finding that DBP was constantly expressed at a high level in the rats with the low-sodium diet, but that the expression of DBP became down-regulated along with the progression of heart failure only in the sodium-loaded rats. It would be an intriguing question whether DBP functions for cardioprotective effect.

In conclusion, our study has provided new insight into the molecular mechanisms of cardiac hypertrophy and heart failure. Additional screening to identify genes whose expression is altered specifically at the heart failure stage should further increase our understanding of this condition.

Acknowledgments

We are grateful to T. Kanbe for her excellent technical assistance. This work was supported in part by a Grant-in-Aid for Scientific Research on Priority Areas (C) "Medical Genome Science" from the Ministry of Education, Science, Sports and Culture of Japan.

References

[1] M.A. James, A.M. Saadeh, J.V. Jones, Wall stress and hypertension, J. Cardiovasc. Risk 7 (2000) 187–190.

[2] E. Braunwald, Shattuck lecture—cardiovascular medicine at the turn of the millennium: triumphs, concerns, and opportunities, New. Engl. J. Med. 337 (1997) 1360–1369.
[3] J. Scheuer, Catecholamines in cardiac hypertrophy, Am. J. Cardiol. 83 (1999) 70H–74H.
[4] J.P. Rapp, S.M. Wang, H. Dene, A genetic polymorphism in the renin gene of Dahl rats cosegregates with blood pressure, Science 243 (1989) 542–544.
[5] D.J. Duggan, M. Bittner, Y. Chen, P. Meltzer, J.M. Trent, Expression profiling using cDNA microarrays, Nat. Genet. 21 (1999) 10–14.
[6] U. Alon, N. Barkai, D.A. Notterman, K. Gish, S. Ybarra, D. Mack, A.J. Levine, Broad patterns of gene expression revealed by clustering analysis of tumor and normal colon tissues probed by oligonucleotide arrays, Proc. Natl. Acad. Sci. USA 96 (1999) 6745–6750.
[7] L.K. Dahl, M. Heine, Primary role of renal homografts in setting chronic blood pressure levels in rats, Circ. Res. 36 (1975) 692–696.
[8] R.B. Sterzel, F.C. Luft, Y. Gao, J. Schnermann, J.P. Briggs, D. Ganten, R. Waldherr, E. Schnabel, W. Kriz, Renal disease and the development of hypertension in salt-sensitive Dahl rats, Kidney Int. 33 (1988) 1119–1129.
[9] K. Yamamoto, T. Masuyama, Y. Sakata, T. Mano, N. Nishikawa, H. Kondo, N. Akehi, T. Kuzuya, T. Miwa, M. Hori, Roles of renin–angiotensin and endothelin systems in development of diastolic heart failure in hypertensive hearts, Cardiovasc. Res. 47 (2000) 274–283.
[10] W. Hayashida, Y. Kihara, A. Yasaka, S. Sasayama, Cardiac calcineurin during transition from hypertrophy to heart failure in rats, Biochem. Biophys. Res. Commun. 273 (2000) 347–351.
[11] Y. Sakata, T. Masuyama, K. Yamamoto, N. Nishikawa, H. Yamamoto, H. Kondo, K. Ono, K. Otsu, T. Kuzuya, T. Miwa, H. Takeda, E. Miyamoto, M. Hori, Calcineurin inhibitor attenuates left ventricular hypertrophy, leading to prevention of heart failure in hypertensive rats, Circulation 102 (2000) 2269–2275.
[12] Y. Iwanaga, Y. Kihara, K. Hasegawa, K. Inagaki, T. Yoneda, S. Kaburagi, M. Araki, S. Sasayama, Cardiac endothelin-1 plays a critical role in the functional deterioration of left ventricles during the transition from compensatory hypertrophy to congestive heart failure in salt-sensitive hypertensive rats, Circulation 98 (1998) 2065–2073.
[13] T. Shioi, A. Matsumori, Y. Kihara, M. Inoko, K. Ono, Y. Iwanaga, T. Yamada, A. Iwasaki, K. Matsushima, S. Sasayama, Increased expression of interleukin-1 beta and monocyte chemotactic and activating factor/monocyte chemoattractant protein-1 in the hypertrophied and failing heart with pressure overload, Circ. Res. 81 (1997) 664–671.
[14] A. Rosenzweig, C.E. Seidman, Atrial natriuretic factor and related peptide hormones, Annu. Rev. Biochem. 60 (1991) 229–255.
[15] R. Natarajan, N. Gonzales, L. Lanting, J. Nadler, Role of the lipoxygenase pathway in angiotensin II-induced vascular smooth muscle cell hypertrophy, Hypertension 23 (1994) 1142–1147.
[16] J.L. Gu, H. Pei, L. Thomas, J.L. Nadler, J.J. Rossi, L. Lanting, R. Natarajan, Ribozyme-mediated inhibition of rat leukocyte-type 12-lipoxygenase prevents intimal hyperplasia in balloon-injured rat carotid arteries, Circulation 103 (2001) 1446–1452.
[17] S.A. Gabel, R.E. London, C.D. Funk, C. Steenbergen, E. Murphy, Leukocyte-type 12-lipoxygenase-deficient mice show impaired ischemic preconditioning-induced cardioprotection, Am. J. Physiol. Heart Circ. Physiol. 280 (2001) 1963–1969.
[18] C. Lasserre, L. Christa, M.T. Simon, P. Vernier, C. Brechot, A novel gene (HIP) activated in human primary liver cancer, Cancer Res. 52 (1992) 5089–5095.
[19] V. Keim, J.L. Iovanna, B. Orelle, J.M. Verdier, M. Busing, U. Hopt, J.C. Dagorn, A novel exocrine protein associated with pancreas transplantation in humans, Gastroenterology 103 (1992) 248–254.
[20] C.R. Mueller, P. Maire, U. Schibler, DBP, a liver-enriched transcriptional activator, is expressed late in ontogeny and its tissue specificity is determined posttranscriptionally, Cell 61 (1990) 279–291.
[21] D.W. Drolet, K.M. Scully, D.M. Simmons, M. Wegner, K.T. Chu, L.W. Swanson, M.G. Rosenfeld, TEF, a transcription factor expressed specifically in the anterior pituitary during embryogenesis, defines a new class of leucine zipper proteins, Genes Dev. 5 (1991) 1739–1753.
[22] T. Inaba, W.M. Roberts, L.H. Shapiro, K.W. Jolly, S.C. Raimondi, S.D. Smith, A.T. Look, Fusion of the leucine zipper gene HLF to the E2A gene in human acute B- lineage leukemia, Science 257 (1992) 531–534.
[23] I.G. Cowell, A. Skinner, H.C. Hurst, Transcriptional repression by a novel member of the bZIP family of transcription factors, Mol. Cell. Biol. 12 (1992) 3070–3077.
[24] S. Ikushima, T. Inukai, T. Inaba, S.D. Nimer, J.L. Cleveland, A.T. Look, Pivotal role for the NFIL3/E4BP4 transcription factor in interleukin 3- mediated survival of pro-B lymphocytes, Proc. Natl. Acad. Sci. USA 94 (1997) 2609–2614.

British Journal of Haematology, 2003, 123, 288–296

DNA microarray analysis of stage progression mechanism in myelodysplastic syndrome

MASUZU UEDA,[1] JUN OTA,[2,3] YOSHIHIRO YAMASHITA,[2] YOUNG LIM CHOI,[2] RURI OHKI,[2] TOMOAKI WADA,[2] KOJI KOINUMA,[2] YASUHIKO KANO,[4] KEIYA OZAWA[1] AND HIROYUKI MANO[2,3] *Divisions of* [1]*Hematology and* [2]*Functional Genomics, Jichi Medical School, Kawachigun, Tochigi,* [3]*CREST, JST, Saitama, and* [4]*Tochigi Cancer Center, Utsunomiya, Tochigi, Japan*

Received 26 May 2003; accepted for publication 30 June 2003

Summary. Myelodysplastic syndrome (MDS) is a clonal disorder of haematopoietic stem cells. Despite the high incidence of MDS in the elderly, effective treatment of individuals in its advanced stages is problematic. DNA microarray analysis is a potentially informative approach to the development of new treatments for MDS. However, a simple comparison of 'transcriptomes' of bone marrow mononuclear cells among individuals at distinct stages of MDS would result in the identification of genes whose expression differences only reflect differences in the proportion of MDS blasts within bone marrow. Such a 'population shift' effect has now been avoided by purification of haematopoietic stem-like cells that are positive for the cell surface marker AC133 from the bone marrow of healthy volunteers and 30 patients at various stages of MDS. Microarray analysis with the $AC133^+$ cells from these individuals resulted in the identification of sets of genes with expression that was specific to either indolent or advanced stages of MDS. The former group of genes included that for PIASy, which catalyses protein modification with the ubiquitin-like molecule SUMO. Induction of PIASy expression in a mouse myeloid cell line induced apoptosis. A loss of PIASy expression may therefore contribute directly to the growth of MDS blasts and stage progression.

Keywords: DNA microarray, myelodysplastic syndrome, haematopoietic stem cell, acute myeloid leukaemia, apoptosis.

Myelodysplastic syndrome (MDS) is a clonal haematological disorder that mainly affects elderly people (Lowenthal & Marsden, 1997) and is characterized by dysplasia in multiple lineages of blood cells, including myeloid, erythroid and megakaryocytic-platelet lineages. MDS is therefore thought to result from the malignant transformation of pluripotent haematopoietic stem cells (HSCs). Another important characteristic of MDS is the co-existence of increased cellularity in bone marrow (BM) and cytopenia in peripheral blood, a condition referred to as 'ineffective haematopoiesis'. Immature BM cells of individuals with MDS may thus be defective with regard to differentiation or undergo apoptosis before giving rise to a sufficient number of progeny.

The clinical course of MDS can be divided into several distinct phases (Harris *et al*, 1999). In the early, indolent stage, affected individuals manifest only cytopenia and may not require any specific treatment; this phase is referred to as 'refractory anaemia' (RA) or 'RA with ringed sideroblasts' (RARS), depending on the absence or presence of ringed sideroblasts in BM. After experiencing the indolent phase for several years (or even decades), a proportion of patients undergoes transformation to a leukaemic state. As the percentage of leukaemic blasts in BM increases, patients are diagnosed first with 'RA with excess blasts' (RAEB) (5–20% blasts in BM) and, finally, with MDS-associated 'acute myeloid leukaemia' (> 20% blasts in BM). The malignant cells of individuals with such MDS-associated leukaemia are refractory to chemotherapy, and the median survival time of these patients is < 1 year.

The development of an effective treatment for MDS will require the characterization of the molecular mechanism that underlies stage progression. Although point mutations in *RAS* proto-oncogenes have been detected in the transformed cells of individuals with MDS, the prognostic value of these mutations is unclear (Horiike *et al*, 1994; Neubauer *et al*, 1994). Allelic loss of the *P53* tumour-suppressor gene and point mutations in the remaining allele have been detected in the advanced stages of MDS, but only in a small

Correspondence: Hiroyuki Mano, Division of Functional Genomics, Jichi Medical School, 3311-1 Yakushiji, Kawachi-gun, Tochigi 329-0498, Japan. E-mail: hmano@jichi.ac.jp

percentage of patients (Fenaux *et al*, 1996). Transcriptional repression through promoter silencing has also been demonstrated in MDS patients for the tumour-suppressor gene that encodes $p15^{INK4b}$ (Quesnel *et al*, 1998). However, none of these gene alterations has been shown to be relevant to stage progression in MDS.

DNA microarray analysis enables the 'transcriptome' of a given cell type or tissue to be monitored. The expression levels of thousands of genes can thus be quantified simultaneously with this technology (Duggan *et al*, 1999). Such large-scale screening offers the possibility of identifying genes whose expression changes in a stage-dependent manner during the clinical course of MDS. The identification of such stage-specific genes would facilitate the molecular diagnosis of MDS and the prediction of stage progression, as well as providing insight into the molecular events that underlie the expansion of leukaemic blasts in individuals with this condition. However, a simple comparison by microarray analysis among BM mononuclear cells (MNCs) derived from patients at different stages of MDS is likely to generate a large number of pseudopositive results, given that the proportion of leukaemic blasts varies widely among such individuals. If, for instance, the transcriptome of BM MNCs is compared between patients with RA and those with MDS-associated leukaemia, the analysis would mistakenly indicate that genes with expression that is specific to immature blood cells are induced in MDS-associated leukaemia. These results would reflect the expansion of the immature leukaemic cell population in the BM of individuals with MDS-associated leukaemia rather than an increase in the mRNA copy number of the corresponding genes per cell.

Such a 'population shift' effect could be prevented by purification of background-matched cell populations from clinical specimens before microarray analysis. Given that malignant transformation occurs in HSCs of individuals with MDS, we hypothesized that HSCs would be a good target for such 'background-matched population' (BAMP) screening (Miyazato *et al*, 2001) of MDS. Analysis of HSCs should thus enable the direct comparison of the transcriptomes of MDS blasts, irrespective of the blast population size within BM or the differentiation capacity of the blasts. To achieve this goal, we took advantage of the HSC-specific surface marker AC133 (Hin *et al*, 1997) and began to purify and store, in a depository known as the 'Blast Bank', AC133-positive HSC-like fractions from individuals with leukaemia or leukaemia-related disorders, including MDS (Miyazato *et al*, 2001). Using Blast Bank cells, we have identified previously genes whose expression helps in the differential diagnosis between MDS-associated leukaemia and *de novo* acute myeloid leukaemia (Miyazato *et al*, 2001). We have also identified genes whose expression is stage dependent in chronic myeloid leukaemia (Ohmine *et al*, 2001).

The expression levels of 2304 genes have now been compared among Blast Bank samples derived from 30 MDS patients (11 with RA, five with RAEB and 14 with MDS-associated leukaemia) and healthy volunteers. We identified a set of genes whose expression was high in cells from control individuals and RA patients but reduced in those from patients at advanced stages of disease. These genes include the one for PIASy, an E3 ligase for the small ubiquitin-like protein known as SUMO and a potential inhibitor of signal transducer and activator of transcription (STAT) 1 (Liu *et al*, 2001). Further investigation revealed that expression of PIASy induced apoptosis in the mouse myeloid cell line 32D (Greenberger *et al*, 1983). A reduction in the level of PIASy expression may therefore contribute to the growth of leukaemic blasts and stage progression in MDS.

PATIENTS AND METHODS

RNA preparation and DNA microarray analysis. $AC133^+$ cells were purified from BM MNCs of MDS patients using MicroBeads conjugated with antibodies to AC133 (Miltenyi Biotec, Auburn, CA, USA), as described previously (Miyazato *et al*, 2001). $AC133^+$ cells were also purified from BM MNCs of two healthy volunteers and then mixed for use as a 'healthy control' sample. Total RNA was extracted from $AC133^+$ cells and subjected to two rounds of amplification with T7 RNA polymerase (Van Gelder *et al*, 1990); the fidelity of the RNA amplification procedure was confirmed as described previously (Ohmine *et al*, 2001). The amplified cRNA (1 μg) was converted to double-stranded cDNA, which was then used to synthesize biotin-labelled cRNA with the ExpressChip labelling system (Mergen, San Leandro, CA, USA). The labelled cRNA was allowed to hybridize both with a DNA microarray (HO-3, Mergen) that contains oligonucleotides based on genes that encode mostly transcription factors as well as with our custom-made array (Mergen) that contains oligonucleotides corresponding to genes for membrane proteins or proteins that mediate cell signalling or redox regulation. The names and database accession numbers for the 2304 genes represented on the arrays are available (Supplementary material, Table SI). Detection of hybridization signals and analysis of the digitized data were performed with a 418 array scanner (Affymetrix, Santa Clara, CA, USA) and GENESPRING 4.1.0 software (Silicon Genetics, Redwood, CA, USA) respectively. In a hierarchical clustering analysis, similarity was measured by the standard correlation with a separation ratio of 0·5.

Real-time polymerase chain reaction (PCR) analysis. Portions of unamplified cDNA were subjected to PCR with SYBR green PCR core reagents (PE Applied Biosystems, Foster City, CA, USA). Incorporation of the SYBR green dye into PCR products was monitored in real time with an ABI Prism 7700 sequence detection system (PE Applied Biosystems), thus allowing determination of the threshold cycle (C_T) at which the exponential amplification of PCR products begins. The C_T values for cDNAs corresponding to the β-actin gene and PIASy were used to calculate the abundance of the PIASy transcript relative to that of β-actin mRNA. The oligonucleotide primers for PCR were as follows: 5′-CCATCATGAAGTGTGACGTGG-3′ and 5′-GTCCGCCTAGAAGCATTTGCG-3′ *for* β-actin cDNA; and 5′-AACTACGGCAAGAGCTACTCGGTG-3′ and 5′-GTTCATCTGCAGGTAGAAGACGGC-3′ for PIASy cDNA.

Conditional expression of PIASy. The mouse myeloid cell line 32D was maintained in Roswell Park Memorial Institute (RPMI)-1640 medium (Life Technologies, Rockville, MD, USA) supplemented with 10% fetal bovine serum (FBS) and interleukin 3 (IL-3; 25 U/ml). For the induction of granulocyte differentiation, cells were cultured in RPMI 1640 supplemented with 10% FBS and 1 ng/ml granulocyte colony-stimulating factor (G-CSF). The cDNA encoding human PIASy (Helix Institute, Chiba, Japan) with a C-terminal FLAG epitope tag (PIASy-F) was inserted into the pMX-tetOFF retroviral vector (Ohmine *et al*, 2001), yielding pMX-tetOFF/PIASy-F. Either pMX-tetOFF or pMX-tetOFF/PIASy-F was then transiently introduced into the packaging cell line BOSC23 (Pear *et al*, 1993) in order to produce the ecotropic retroviruses MX-tetOFF and MX-tetOFF/PIASy-F respectively. 32D cells were then infected with the virus-containing supernatant of BOSC23 cells for 24 h in the presence of retronectin (Takara Shuzo, Shiga, Japan). The cells were subsequently harvested and cultured in RPMI 1640–FBS–IL-3 medium supplemented with blasticidin-S (5 μg/ml; Funakoshi, Tokyo, Japan) and tetracycline (1 μg/ml; Boehringer Mannheim, Mannheim, Germany). The expression of PIASy-F was induced by changing the culture medium to RPMI 1640 supplemented with 10% FBS, 2 μmol/l 17β-oestradiol (Sigma, St Louis, MO, USA) and appropriate cytokines.

Protein analysis was performed as described previously (Ohmine *et al*, 2001). Total-cell lysates (10 μg per lane) were fractionated by 7·5% sodium dodecyl sulphate polyacrylamide gel electrophoresis (SDS-PAGE) and subjected to immunoblot analysis with antibodies to FLAG (Eastman Kodak, New Haven, CT, USA).

Apoptosis of 32D cells. 32D cells infected with MX-tetOFF or MX-tetOFF/PIASy-F were cultured for 8 d in the presence of G-CSF and 17β-oestradiol, after which the cells were stained with Wright–Giemsa solution or with propidium iodide (PI) and fluorescein isothiocyanate (FITC)-conjugated annexin V (annexin V–FITC apoptosis detection kit; BD Biosciences, San Jose, CA, USA) in order to evaluate apoptotic changes with a FACScan processor (BD Biosciences). Differentiation of 32D cells was evaluated by FACScan processor analysis with antibodies to the granulocyte-specific marker Gr-1 (BD Biosciences).

RESULTS

Transcriptome analysis of MDS samples

For this analysis, we prepared a custom-made microarray that contains oligonucleotides corresponding to a total of 1152 human genes encoding for membrane proteins and proteins involved in redox regulation or cell signalling. Membrane proteins were chosen because diagnosis by flow cytometry with antibodies to MDS-specific cell surface markers, if found, would be of great clinical value. We also reasoned that, from the point of view of resistance mechanisms to chemotherapeutic reagents, cell surface proteins as well as those involved in redox regulation should be focused on.

Many cases of disease-specific chromosome translocation found in leukaemias lead to deregulation in the expression of transcriptional factors or to the generation of fusion products containing the transcriptional factors as the components (Alcalay *et al*, 2001). These data suggest an important role for the altered functions of transcriptional factors in leukaemogenesis. We therefore used a commercially available microarray (HO3) containing oligonucleotides based on 1152 genes encoding mainly transcriptional factors.

The expression profile for a total of 2304 genes was thus obtained for Blast Bank samples purified from 11 patients with RA, five patients with RAEB and 14 patients with MDS-associated leukaemia. The pooled $AC133^+$ cells from two healthy volunteers were used as a healthy control sample. Expression intensity data for the various genes were normalized relative to the median expression value of all genes in each hybridization. The resulting data were then used to generate a dendrogram, or 'gene tree', in which genes with similar expression profiles were clustered near each other (Fig 1A). About 50% of the genes analysed were transcriptionally silent throughout the clinical course of MDS. Several clusters of genes, however, were expressed in a manner dependent on MDS stage. For example, genes in the cluster designated #1 were highly expressed only in RA patients 3 and 7, whereas those in cluster #2 were expressed at a higher level in patients with RAEB or MDS-associated leukaemia than in healthy controls or RA patients. These genes were thus potential molecular markers for the corresponding MDS stage.

To facilitate the identification of genes that are expressed in a stage-dependent manner, we calculated the mean expression value of each gene for RA, RAEB and MDS-associated leukaemia groups and then used these values to generate another dendrogram, an 'average tree' (Fig 1B). From the resulting, readily identifiable, gene clusters with stage-specific expression profiles, we then attempted to select those genes with stage-dependent expression that was statistically significant by Welch analysis of variance (ANOVA). However, most genes whose stage-dependent expression was significant ($P < 0{\cdot}001$) were found not to be appropriate stage-specific markers. Such analysis thus tended to select genes whose expression level exhibited a small deviation within each MDS stage; the expression intensities for these genes, however, did not exhibit large differences among disease stages.

Genes induced during stage progression

An important goal of this study was to clarify the molecular events that underlie the progression from indolent RA to therapy-refractory RAEB and MDS-associated leukaemia. We thus focused our attention on identifying differences in the transcriptome between disease stages with good prognosis (healthy control and RA) and those with poor prognosis (RAEB and MDS-associated leukaemia). The mean expression intensity of each gene was thus calculated for the good prognosis group and the poor prognosis group, and the differences in the resulting values are represented in Fig 1C.

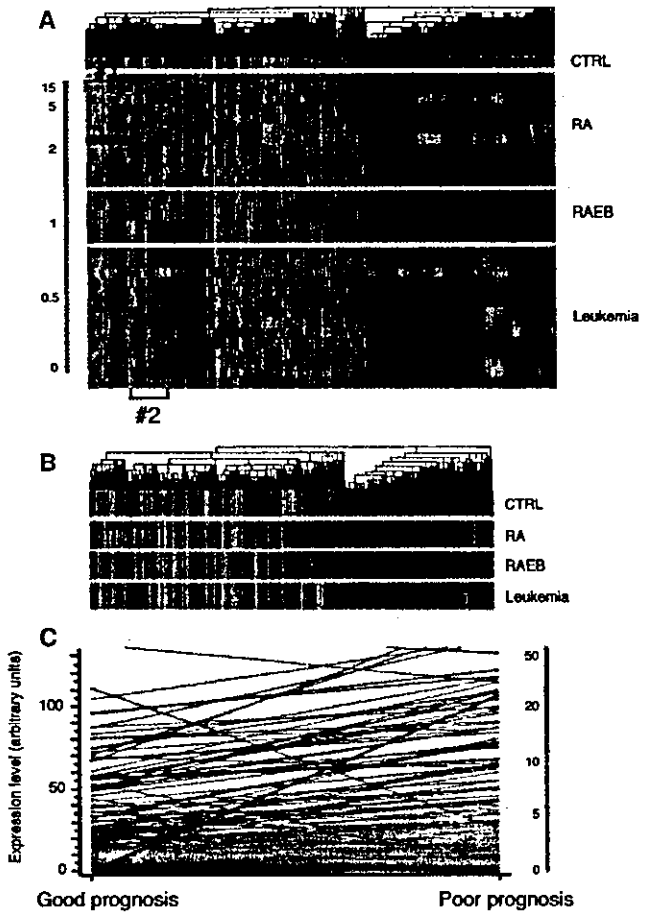

Fig 1. Expression profiles of 2304 genes in the MDS blasts. (A) Hierarchical clustering of 2304 genes on the basis of their expression profiles in Blast Bank samples derived from healthy controls (CTRL) and 30 individuals with MDS [11 with RA, five with RAEB and 14 with MDS-associated leukaemia (Leukaemia)]. Each column represents a single gene on the microarray, and each row a separate patient (or control) sample. The fluorescence intensity of each gene was normalized relative to the median fluorescence value for all spots in each hybridization, and the normalized value is colour-coded as indicated on the left. The positions of clusters of RA-specific genes (cluster #1) and of RAEB- or MDS-associated leukaemia-specific genes (cluster #2) are indicated. (B) The mean expression levels of each gene were calculated for RA, RAEB and MDS-associated leukaemia groups and then used to generate another dendrogram, or 'average tree.' Clusters of genes whose expression was specific to different groups are evident. (C) Comparison of gene expression levels between good prognosis (healthy control and RA) and poor prognosis (RAEB and MDS-associated leukaemia) groups. The mean expression values of each gene were calculated for the good prognosis and bad prognosis groups and then compared between the two groups. Each line corresponds to a single gene and is coloured according to the mean expression level of the gene in the good prognosis group. The hypothetical 'poor prognosis-specific gene' is shown in blue.

We first attempted to identify genes with expression that was induced in the AC133$^+$ cells of the poor prognosis group, compared with that in the corresponding cells of the good prognosis group. The GENESPRING software was used to search for genes whose expression profiles were statistically similar, with a minimum correlation of 0·99, to that of a hypothetical 'poor prognosis-specific gene' (blue line in Fig 1C) that exhibits a mean expression level of 0·0 arbitrary units (U) in the good prognosis group and 100·0 U in the poor prognosis group. From a total of 96 such genes, we then selected those whose expression level was < 20·0 U in all samples from the good prognosis group and > 50·0 U in at least one sample from the poor prognosis group.

Eleven such genes were finally identified (Fig 2A), including those for NADH-ubiquinone oxidoreductase flavoprotein 1 (NDUFV1), LIM-Hox2 (LH2) and paraneoplastic antigen MA2 (PNMA2). Expression of *NDUFV1*, for example, was highly specific to the poor prognosis group: its expression level was 4·60, 1·50 ± 0·92, 26·29 ± 11·30 and 10·36 ± 9·04 U (means ± standard deviation, SD) for the control, RA, RAEB and MDS-associated leukaemia samples respectively. The difference in *NDUFV1* expression level between the good and poor prognosis groups was statistically significant ($P = 0·0061$, Mann–Whitney *U*-test). NDUFV1 is a component of NADH:ubiquinone oxidoreductase, which participates in mitochondrial electron transport (Ali *et al*, 1993). Increased expression of *NDUFV1* may therefore reflect an increased rate of mitochondrial respiration in the transformed blast cells.

LH2 is a homeobox-containing transcription factor. Although neither its target genes nor its *in vivo* functions have been identified, LH2 has been suggested to participate in mitogenic signalling on the basis of the observations that the corresponding gene is aberrantly expressed in chronic myeloid leukaemia (Wu *et al*, 1996) and that the protein is expressed in immature, but not in mature, B lymphocytes (Xu *et al*, 1993). PNMA2 was originally identified as a serological marker produced by testicular cancer cells (Voltz *et al*, 1999) and may function as an antigen that causes paraneoplastic syndromes. Expression of these three genes only in the advanced stages of MDS may provide a basis for the differential diagnosis of MDS at the molecular level.

Genes silenced during stage progression

Given the importance of functional deficiency of various tumour-suppressor genes in malignant transformation, a

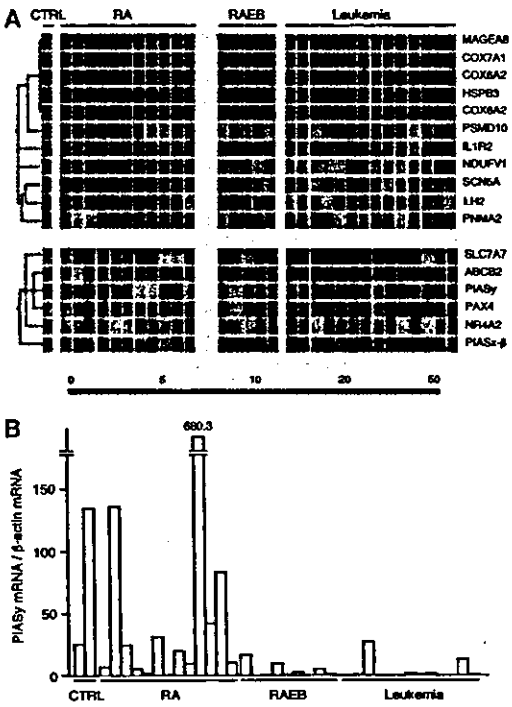

Fig 2. Identification of stage-dependent genes. (A) The expression profiles of 11 poor prognosis-specific genes (top) and six good prognosis-specific genes (bottom) are shown colour-coded as indicated by the scale below. Each row corresponds to a single gene, with the columns indicating the corresponding expression level in AC133$^+$ cells obtained from healthy controls (CTRL) or individual RA, RAEB and MDS-associated leukaemia (Leukaemia) patients. The similarity of expression profiles among the poor prognosis-specific or the good prognosis-specific genes is indicated by the purple or blue dendrogram, respectively, shown on the left. The names, accession numbers and expression intensity data for the genes are available (Supplementary material, Tables SII and SIII). (B) Quantification of *PIASy* transcripts in AC133$^+$ blasts. Complementary DNA was prepared from the blasts of 37 individuals, comprising two healthy volunteers (CTRL) as well as 13 RA, nine RAEB and 13 MDS-associated leukaemia (Leukaemia) patients, and was subjected to real-time PCR analysis with the primers specific for *PIASy* or the β-actin gene. The ratio of the abundance of *PIASy* transcripts to that of β-actin mRNA was calculated as 2^n, where n is the C_T value for β-actin cDNA minus the C_T value of *PIASy* cDNA.

decrease in the expression of certain genes may contribute directly to stage progression in MDS. We therefore searched for genes whose expression profiles were statistically similar to that of a hypothetical 'good prognosis-specific gene' that exhibits a mean expression level of 100·0 U in the good prognosis group and 0·0 U in the poor prognosis group. A total of 182 such genes were identified. We then selected those genes with an expression level of > 40·0 U in at least one sample from the good prognosis group and of < 20·0 U in all samples from the poor prognosis group; six such genes were finally identified (Fig 2A).

Among these six genes were those for PIASy and PIASx-β, members of the PIAS family of signalling proteins (Shuai, 2000). PIASy was identified as a binding protein and inhibitor of STAT1 (Liu *et al*, 2001). More recent studies have indicated that PIAS proteins perform a wide spectrum of functions, including modification of the activity of the androgen receptor (Gross *et al*, 2001) or p53 (Nelson *et al*, 2001) and sumoylation of the transcription factor LEF1 (Sachdev *et al*, 2001). Moreover, forced expression of PIASy in human kidney 293T cells was shown to be accompanied by induction of apoptosis (Liu & Shuai, 2001), suggesting that PIASy also possesses proapoptotic activity. Our data indicated that *PIASy* is active in normal HSCs or pluripotent stem cells in the indolent stage of MDS, but that expression of the gene is suppressed in these cells on transition to the advanced stages of MDS. If the proapoptotic activity of PIASy is required *in vivo* to prevent deregulation of the growth of HSCs in normal individuals or RA patients, then the loss of *PIASy* expression may allow the accelerated growth of blastic cells within BM, the hallmark of RAEB and MDS-associated leukaemia. The expression level of *PIASy* may thus not only prove useful as a molecular marker for stage diagnosis or prediction of prognosis in individuals with MDS but could also contribute directly to the mechanism of transformation to the advanced stages of this disease.

We therefore attempted to verify the stage-dependent expression of *PIASy* by quantitative real-time PCR analysis. The abundance of *PIASy* transcripts was determined relative to that of β-actin mRNA in the AC133$^+$ blasts from 37 individuals, including two healthy volunteers as well as 13 RA, nine RAEB and 13 MDS-associated leukaemia patients. Consistent with the results obtained by microarray analysis, PCR showed that the expression of *PIASy* was markedly greater in the blasts from control subjects or RA patients compared with that in those from RAEB or MDS-associated leukaemia patients ($P = 0{\cdot}043$, Mann–Whitney U-test) (Fig 2B). *PIASy* is thus a potential candidate for a stage-dependent molecular marker in MDS.

Inhibition of 32D cell growth by overexpression of PIASy

Given the potential proapoptotic activity of PIASy, sustained expression of the corresponding gene might influence the growth or differentiation of immature blood cells. To examine directly the effect of *PIASy* expression in such cells, we took advantage of the pMX-tetOFF retrovirus vector (Ohmine *et al*, 2001), which allows the dual regulation of exogenous gene expression by tetracycline and β-oestradiol (Iida *et al*, 1996). The mouse myeloid cell line 32D grows without differentiation in the presence of IL-3, but exhibits a reduction in growth rate and undergoes terminal differentiation to granulocytes in response to stimulation with G-CSF. We therefore infected 32D cells with the viruses MX-tetOFF or MX-tetOFF/PIASy-F, the latter of which encodes FLAG epitope-tagged PIASy, and maintained the cells under non-inducing (presence of tetracycline, absence of β-oestradiol) or inducing (minus tetracycline, plus β-oestradiol) conditions with regard to PIASy-F expression. Immunoblot analysis with antibodies to the FLAG epitope revealed the expression of PIASy-F at a high level only in the cells that were infected with

MX-tetOFF/PIASy-F and maintained under the inducing condition (Fig 3A).

The effect of PIASy expression on cell growth was examined in virus-infected 32D cells cultured in the presence of IL-3. No difference in cell growth, viability, morphology or surface marker expression was apparent between cells infected with MX-tetOFF/PIASy-F that were maintained under inducing conditions and those that were cultured under non-inducing conditions (data not shown).

We next examined the effect of PIASy expression on virus-infected cells cultured in the presence of G-CSF. Under the non-inducing condition, both mock-infected and MX-tetOFF/PIASy-F-infected cells grew in a similar manner (Fig 3B). The induction of PIASy-F expression, however, resulted in growth inhibition. Although β-oestradiol exhibited a slight inhibitory effect on the growth of the mock-infected cells, the effect of this agent on the MX-tetOFF/PIASy-F-infected cells was markedly greater. Concomitant with its inhibitory effect on cell growth, PIASy-F expression induced a substantial decrease in cell viability (Fig 3B).

PIASy-induced apoptosis in 32D cells

To clarify the mechanism by which PIASy inhibits the growth and reduces the viability of 32D cells in the presence of G-CSF, we examined the morphology of cells maintained for 8 d under inducing conditions by staining with Wright–Giemsa solution (Fig 4A). Mock-infected cells cultured in the presence of IL-3 were of medium to large size and exhibited a high nucleus-to-cytoplasm ratio. When cultured in the presence of G-CSF, > 50% of the mock-infected cells displayed the differentiated phenotype; some cells thus had a lower nucleus-to-cytoplasm ratio and neutrophilic cytoplasm and, in others, the nucleus was segmented. In the presence of IL-3, cells expressing PIASy-F showed a phenotype similar to that of the mock-infected cells. Culture of the cells expressing PIASy-F in the presence of G-CSF, however,

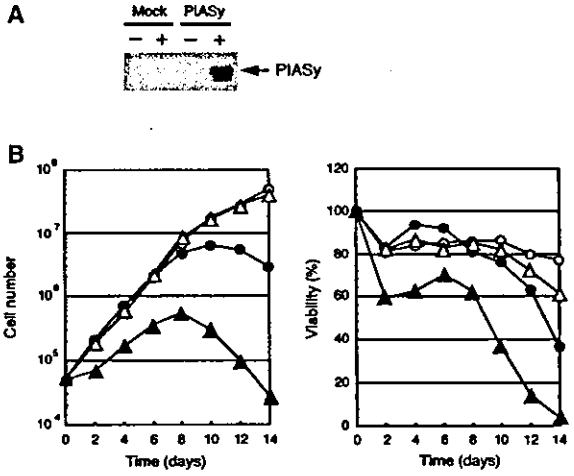

Fig 3. Effects of PIASy expression on cell growth and viability. (A) 32D cells were infected with MX-tetOFF (mock) or MX-tetOFF/PIASy-F (PIASy) retroviruses and cultured in the presence of IL-3, blasticidin-S and tetracycline. The blasticidin-S-resistant mass culture was then maintained overnight under the same condition (–) or in medium containing β-oestradiol instead of tetracycline (+), after which the cells were harvested and subjected to immunoblot analysis with antibodies to the FLAG tag. (B) 32D cells infected with MX-tetOFF (circles) or MX-tetOFF/PIASy-F (triangles) were cultured in the presence of G-CSF under either non-inducing (open symbols) or inducing (closed symbols) conditions. Total cell number (left) and cell viability assessed on the basis of trypan blue exclusion (right) were determined at the indicated times. Data are means of triplicates from a representative experiment.

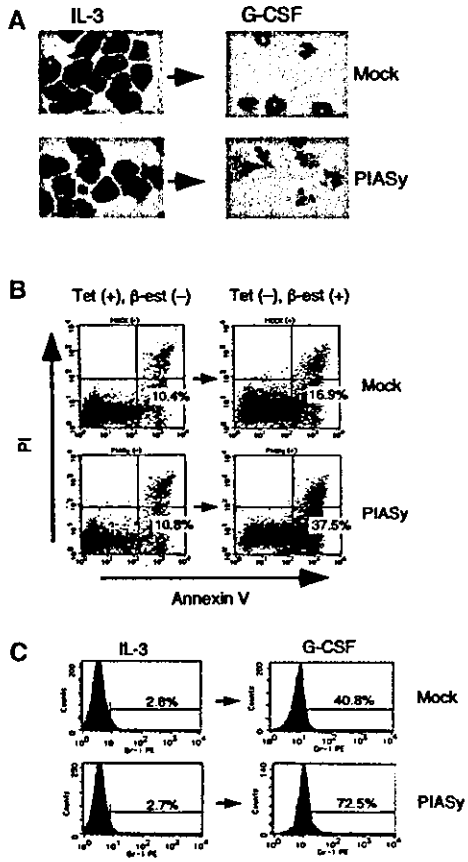

Fig 4. Induction of apoptosis by PIASy. (A) 32D cells infected with MX-tetOFF (mock) or MX-tetOFF/PIASy-F (PIASy) were incubated for 8 d under the inducing condition in the presence of either IL-3 or G-CSF, as indicated. The cells were then stained with Wright–Giemsa solution. Original magnification, 200 ×. (B) 32D cells infected with MX-tetOFF or MX-tetOFF/PIASy-F were incubated for 8 d with G-CSF under the non-inducing [Tet (+), β-est (–)] or inducing [Tet (–), β-est (+)] condition. They were then stained with annexin V–FITC and PI and subjected to flow cytometry. The percentages of apoptotic cells (annexin V-positive, PI-negative) are indicated. (C) 32D cells infected with MX-tetOFF or MX-tetOFF/PIASy-F were cultured under the inducing condition in the presence of either IL-3 or G-CSF. The proportion of differentiated cells was then evaluated by flow cytometry with phycoerythrin–conjugated antibodies to the granulocyte-specific marker Gr-1. The percentages of Gr-1$^+$ cells are indicated.

resulted in a marked increase in the number of cells with apoptotic characteristics, including condensation and fragmentation of nuclei and cell shrinkage.

To determine the extent of apoptosis induction by PIASy in 32D cells cultured in the presence of G-CSF, we subjected cells that had been incubated for 8 d with this cytokine to staining with annexin-V and PI. The translocation of phosphatidylserine from the inner leaflet to the outer leaflet of the lipid bilayer of the cell membrane, a characteristic of apoptosis, was then evaluated by flow cytometry. When mock-infected 32D cells were cultured with G-CSF under non-inducing or inducing conditions, 10·4% or 16·9%, respectively, of the cells were characterized as apoptotic (phosphatidylserine-positive, PI-negative). Expression of PIASy-F in cells cultured with G-CSF increased the proportion of apoptotic cells from 10·8% to 37·5% (Fig 4B). The proportion of all dead cells (phosphatidylserine-positive, PI-negative or -positive) was 15·5%, 23·8%, 18·4% or 49·8% for the non-induced mock-infected cells, induced mock-infected cells, non-induced MX-tetOFF/PIASy-F-infected cells and induced MX-tetOFF/PIASy-F-infected cells respectively. These data thus support the notion that PIASy inhibits the growth of differentiating 32D cells through the induction of apoptosis.

To determine whether PIASy expression also promotes the differentiation of 32D cells, we measured the proportion of differentiated cells by flow cytometry with antibodies to the granulocyte-specific surface protein Gr-1. When cultured in the presence of IL-3 under inducing conditions, the proportion of mock-infected or MX-tetOFF/PIASy-F-infected cells that were positive for Gr-1 was < 3% (Fig 4C). Incubation with G-CSF resulted in expansion of the Gr-1$^+$ population in both mock-infected (40·8%) and MX-tetOFF/PIASy-F-infected (72·5%) cells, with the effect in the latter cells being more marked. The peak fluorescence intensities were similar, however, for the mock-infected and MX-tetOFF/PIASy-F-infected cells, suggesting that a relative decrease in the size of the Gr-1$^-$ fraction of PIASy-F-positive cells (probably as a result of apoptosis) may have contributed to the overall increase in the percentage of Gr-1$^+$ cells. Examination of cell morphology by Wright–Giemsa staining also revealed that the time courses for the detection of terminal granulocytes with segmented nuclei were similar for the two groups of infected cells (data not shown). The principal mechanism by which PIASy inhibits 32D cell growth thus appeared to be the induction of apoptosis rather than the acceleration of cell differentiation.

DISCUSSION

In the present study, we purified the AC133$^+$, HSC-like fraction from a large number of MDS patients (including those with MDS-associated leukaemia) and used these cell preparations to compare the expression profiles of genes for cell surface proteins, signalling molecules and transcription factors. We have shown previously that such BAMP screening with purified blasts yields fewer pseudopositive results than do comparisons of MNC preparations (Miyazato *et al*, 2001; Ohmine *et al*, 2001). The BAMP screening applied here to MDS resulted in the identification of sets of stage-specific genes, one of which is the gene for PIASy. The association of the loss of *PIASy* expression with advanced stages of MDS suggests that PIASy functions as a tumour suppressor and prevents stage progression in MDS.

To provide further support for this hypothesis, we examined the effects of PIASy overexpression in the mouse myeloid cell line 32D. The induction of PIASy expression in these cells incubated in the presence of G-CSF resulted in apoptotic cell death. The PIAS family of proteins has been shown previously to induce apoptosis through the activation of c-Jun N-terminal kinase (JNK) 1 (Liu & Shuai, 2001). However, we did not detect any effect of PIASy overexpression on the activity of JNK1 in 32D cells (data not shown). Furthermore, PIASy-induced apoptosis in 32D cells was not prevented by the forced expression of a dominant-negative form of JNK1 (data not shown). It is therefore unlikely that JNK1 is a principal mediator of PIASy-induced apoptosis in these cells.

It was also possible that PIASy affects cell viability through the inhibition of STAT proteins (Liu *et al*, 2001). However, an electrophoretic mobility shift assay did not reveal any inhibition of STAT1 activity by PIASy in 32D cells (data not shown). Moreover, our observation that the G-CSF-induced differentiation of 32D cells was not inhibited by PIASy suggests that the intracellular signalling pathway involving the G-CSF receptor and STAT1 was, at least partially, intact.

Both PIASy and PIAS1 have been shown to function as E3 ligases for SUMO (Kahyo *et al*, 2001; Sachdev *et al*, 2001), as has a yeast PIAS-related protein (Johnson & Gupta, 2001; Takahashi *et al*, 2001). SUMO is a ubiquitin-like molecule that is conjugated to a variety of proteins including RanGAP1, PML, IκB-α and p53 (Hay, 2001). Although, like ubiquitin conjugation, modification with SUMO appears to control the proteolysis of target proteins, sumoylation may also play additional regulatory roles. Given the diversity of sumoylated proteins, the various actions of PIASy described to date may be the result of PIASy-mediated sumoylation. The phenotype associated with PIASy expression may thus depend on the cellular context and the expression of PIASy substrates. The identification of binding partners of PIASy in 32D cells might provide important insight into the molecular mechanism of PIASy-induced apoptosis in these cells.

In conclusion, our microarray analysis with purified Blast Bank samples is an efficient system for the identification of molecular markers for the various stages of MDS. Furthermore, this analysis has yielded important information on the molecular mechanism of transformation in this disease.

ACKNOWLEDGMENTS

We thank A. Iida, J.-K. Yee and T. Kitamura for kindly providing the components used to construct pMX-tetOFF. This work was supported in part by grants for Research on the Human Genome, Tissue Engineering and Food Biotechnology, for the Second-Term Comprehensive 10-Year Strategy for Cancer Control, and for Research on Develop-

ment of Novel Therapeutic Modalities for Myelodysplastic Syndrome from the Ministry of Health, Labor, and Welfare of Japan: by a grant from the Research Foundation for Community Medicine of Japan, the Sankyo Foundation of Life Science, the Takeda Science Foundation and the Mitsubishi Pharma Research Foundation.

SUPPLEMENTARY MATERIAL

The following material is available from http://www.blackwellpublishing.com/products/journals/suppmat/bjh/bjh4601/bjh4601sm.htm

Table SI. The names and GenBank accession numbers for the genes observed on our custom-made array.

Table SII. Expression intensity of the genes suppressed in the advanced stages of MDS.

Table SIII. Expression intensity of the genes activated in the advanced stages of MDS.

REFERENCES

Alcalay, M., Orleth, A., Sebastiani, C., Meani, N., Chiaradonna, F., Casciari, C., Sciurpi, M.T., Gelmetti, V., Riganelli, D., Minucci, S., Fagioli, M. & Pelicci, P.G. (2001) Common themes in the pathogenesis of acute myeloid leukemia. *Oncogene*, 20, 5680–5694.

Ali, S.T., Duncan, A.M., Schappert, K., Heng, H.H., Tsui, L.C., Chow, W. & Robinson, B.H. (1993) Chromosomal localization of the human gene encoding the 51-kDa subunit of mitochondrial complex I (NDUFV1) to 11q13. *Genomics*, 18, 435–439.

Duggan, D.J., Bittner, M., Chen, Y., Meltzer, P. & Trent, J.M. (1999) Expression profiling using cDNA microarrays. *Nature Genetics*, 21, 10–14.

Fenaux, P., Morel, P. & Lai, J.L. (1996) Cytogenetics of myelodysplastic syndromes. *Seminars in Hematology*, 33, 127–138.

Greenberger, J.S., Sakakeeny, M.A., Humphries, R.K., Eaves, C.J. & Eckner, R.J. (1983) Demonstration of permanent factor-dependent multipotential (erythroid/neutrophil/basophil) hematopoietic progenitor cell lines. *Proceedings of the National Academy of Sciences of the USA*, 80, 2931–2935.

Gross, M., Liu, B., Tan, J., French, F.S., Carey, M. & Shuai, K. (2001) Distinct effects of PIAS proteins on androgen-mediated gene activation in prostate cancer cells. *Oncogene*, 20, 3880–3887.

Harris, N.L., Jaffe, E.S., Diebold, J., Flandrin, G., Muller-Hermelink, H.K., Vardiman, J., Lister, T.A. & Bloomfield, C.D. (1999) World Health Organization classification of neoplastic diseases of the hematopoietic and lymphoid tissues: report of the Clinical Advisory Committee meeting, Airlie House, Virginia, November 1997. *Journal of Clinical Oncology*, 17, 3835–3849.

Hay, R.T. (2001) Protein modification by SUMO. *Trends in Biochemical Sciences*, 26, 332–333.

Hin, A.H., Miraglia, S., Zanjani, E.D., Almeida-Porada, G., Ogawa, M., Leary, A.G., Olweus, J., Kearney, J. & Buck, D.W. (1997) AC133, a novel marker for human hematopoietic stem and progenitor cells. *Blood*, 90, 5002–5012.

Horiike, S., Misawa, S., Nakai, H., Kaneko, H., Yokota, S., Taniwaki, M., Yamane, Y., Inazawa, J., Abe, T. & Kashima, K. (1994) N-ras mutation and karyotypic evolution are closely associated with leukemic transformation in myelodysplastic syndrome. *Leukemia*, 8, 1331–1336.

Iida, A., Chen, S.-T., Friedmann, T. & Yee, J.-K. (1996) Inducible gene expression by retrovirus-mediated transfer of a modified tetracycline-regulated system. *Journal of Virology*, 70, 6054–6059.

Johnson, E.S. & Gupta, A.A. (2001) An E3-like factor that promotes SUMO conjugation to the yeast septins. *Cell*, 106, 735–744.

Kahyo, T., Nishida, T. & Yasuda, H. (2001) Involvement of PIAS1 in the sumoylation of tumor suppressor p53. *Molecular Cell*, 8, 713–718.

Liu, B. & Shuai, K. (2001) Induction of apoptosis by protein inhibitor of activated Stat1 through c-Jun NH2-terminal kinase activation. *Journal of Biological Chemistry*, 276, 36624–36631.

Liu, B., Gross, M., ten Hoeve, J. & Shuai, K. (2001) A transcriptional corepressor of Stat1 with an essential LXXLL signature motif. *Proceedings of the National Academy of Sciences of the USA*, 98, 3203–3207.

Lowenthal, R.M. & Marsden, K.A. (1997) Myelodysplastic syndromes. *International Journal of Hematology*, 65, 319–338.

Miyazato, A., Ueno, S., Ohmine, K., Ueda, M., Yoshida, K., Yamashita, Y., Kaneko, T., Mori, M., Kirito, K., Toshima, M., Nakamura, Y., Saito, K., Kano, Y., Furusawa, S., Ozawa, K. & Mano, H. (2001) Identification of myelodysplastic syndrome-specific genes by DNA microarray analysis with purified hematopoietic stem cell fraction. *Blood*, 98, 422–427.

Nelson, V., Davis, G.E. & Maxwell, S.A. (2001) A putative protein inhibitor of activated STAT (PIASy) interacts with p53 and inhibits p53-mediated transactivation but not apoptosis. *Apoptosis*, 6, 221–234.

Neubauer, A., Greenberg, P., Negrin, R., Ginzton, N. & Liu, E. (1994) Mutations in the ras proto-oncogenes in patients with myelodysplastic syndromes. *Leukemia*, 8, 638–641.

Ohmine, K., Ota, J., Ueda, M., Ueno, S.-I., Yoshida, K., Yamashita, Y., Kirito, K., Imagawa, S., Nakamura, Y., Saito, K., Akutsu, M., Mitani, K., Kano, Y., Komatsu, N., Ozawa, K. & Mano, H. (2001) Characterization of stage progression in chronic myeloid leukemia by DNA microarray with purified hematopoietic stem cells. *Oncogene*, 20, 8249–8257.

Pear, W.S., Nolan, G.P., Scott, M.L. & Baltimore, D. (1993) Production of high-titer helper-free retroviruses by transient transfection. *Proceedings of the National Academy of Sciences of the USA*, 90, 8392–8396.

Quesnel, B., Guillerm, G., Vereecque, R., Wattel, E., Preudhomme, C., Bauters, F., Vanrumbeke, M. & Fenaux, P. (1998) Methylation of the p15 (INK4b) gene in myelodysplastic syndromes is frequent and acquired during disease progression. *Blood*, 91, 2985–2990.

Sachdev, S., Bruhn, L., Sieber, H., Pichler, A., Melchior, F. & Grosschedl, R. (2001) PIASy, a nuclear matrix-associated SUMO E3 ligase, represses LEF1 activity by sequestration into nuclear bodies. *Genes and Development*, 15, 3088–3103.

Shuai, K. (2000) Modulation of STAT signaling by STAT-interacting proteins. *Oncogene*, 19, 2638–2644.

Takahashi, Y., Kahyo, T., Toh, E.A., Yasuda, H. & Kikuchi, Y. (2001) Yeast Ull1/Siz1 is a novel SUMO1/Smt3-ligase for septin components and functions as an adaptor between conjugating enzyme and substrates. *Journal of Biological Chemistry*, 276, 48973–48977.

Van Gelder, R.N., von Zastrow, M.E., Yool, A., Dement, W.C., Barchas, J.D. & Eberwine, J.H. (1990) Amplified RNA synthesized from limited quantities of heterogeneous cDNA. *Proceedings of the National Academy of Sciences of the USA*, 87, 1663–1667.

Voltz, R., Gultekin, S.H., Rosenfeld, M.R., Gerstner, E., Eichen, J., Posner, J.B. & Dalmau, J. (1999) A serologic marker of paraneoplastic limbic and brain-stem encephalitis in patients with testicular cancer. *New England Journal of Medicine*, 340, 1788–1795.

Wu, H.K., Heng, H.H., Siderovski, D.P., Dong, W.F., Okuno, Y., Shi, X.M., Tsui, L.C. & Minden, M.D. (1996) Identification of a human LIM-Hox gene, hLH-2, aberrantly expressed in chronic myelogenous leukaemia and located on 9q33–34.1. *Oncogene*, **12**, 1205–1212.

Xu, Y., Baldassare, M., Fisher, P., Rathbun, G., Oltz, E.M., Yancopoulos, G.D., Jessell, T.M. & Alt, F.W. (1993) LH-2: a LIM/homeodomain gene expressed in developing lymphocytes and neural cells. *Proceedings of the National Academy of Sciences of the USA*, **90**, 227–231.

Gα12 activates Rho GTPase through tyrosine-phosphorylated leukemia-associated RhoGEF

Nobuchika Suzuki*, Susumu Nakamura*, Hiroyuki Mano†, and Tohru Kozasa*‡

*Department of Pharmacology, University of Illinois, Chicago, IL 60612; and †Division of Functional Genomics, Jichi Medical School, Tochigi 329-0498, Japan

Edited by Alfred G. Gilman, University of Texas Southwestern Medical Center, Dallas, TX, and approved November 27, 2002 (received for review July 8, 2002)

Heterotrimeric G proteins, G12 and G13, have been shown to transduce signals from G protein-coupled receptors to activate Rho GTPase in cells. Recently, we identified p115RhoGEF, one of the guanine nucleotide exchange factors (GEFs) for Rho, as a direct link between Gα13 and Rho [Kozasa, T., *et al.* (1998) *Science* 280, 2109–2111; Hart, M. J., *et al.* (1998) *Science* 280, 2112–2114]. Activated Gα13 stimulated the RhoGEF activity of p115 through interaction with the N-terminal RGS domain. However, Gα12 could not activate Rho through p115, although it interacted with the RGS domain of p115. The biochemical mechanism from Gα12 to Rho activation remained unknown. In this study, we analyzed the interaction of leukemia-associated RhoGEF (LARG), which also contains RGS domain, with Gα12 and Gα13. RGS domain of LARG demonstrated Gα12- and Gα13-specific GAP activity. LARG synergistically stimulated SRF activation by Gα12 and Gα13 in HeLa cells, and the SRF activation by Gα12-LARG was further stimulated by coexpression of Tec tyrosine kinase. It was also found that LARG is phosphorylated on tyrosine by Tec. In reconstitution assays, the RhoGEF activity of nonphosphorylated LARG was stimulated by Gα13 but not Gα12. However, when LARG was phosphorylated by Tec, Gα12 effectively stimulated the RhoGEF activity of LARG. These results demonstrate the biochemical mechanism of Rho activation through Gα12 and that the regulation of RhoGEFs by heterotrimeric G proteins G12/13 is further modulated by tyrosine phosphorylation.

Members of the Rho family GTPases (Rho, Rac, and Cdc42) regulate a variety of cellular activities such as cell-cycle progression, chemotaxis, or axonal guidance by controlling actin cytoskeletal rearrangements or gene expression (1). Activation of Rho family GTPases is catalyzed by their guanine nucleotide exchange factors (GEFs). These GEFs share a Dbl homology domain and an adjacent pleckstrin homology domain (2). The Dbl homology domain is responsible for the capacity to stimulate GDP–GTP exchange of Rho family GTPases. Except for this common Dbl homology–pleckstrin homology structure, these GEFs contain various protein motifs that are implicated in signal transduction. However, the biochemical mechanism of regulation of these GEFs by upstream signals has been poorly understood.

Heterotrimeric G proteins G12 and G13 have been shown to mediate signals from G protein-coupled receptors to Rho GTPase activation (3–5). Recently, we identified p115RhoGEF, one of GEFs for Rho, as a direct link between heterotrimeric G13 and Rho (6, 7). Activated Gα13 stimulated the RhoGEF activity of p115 through the interaction with the N-terminal RGS (regulator of G protein signaling) domain. However, Gα12 did not activate Rho through p115 in reconstitution assays. Although the overexpression of a constitutively active mutant of Gα12 has demonstrated several evidences supporting Rho activation in cells (5, 8), the biochemical mechanism from Gα12 to Rho activation has not been understood.

Recently, several reports indicated the involvement of tyrosine phosphorylation in the regulation of GEF activity for Rho family GTPases. Tyrosine phosphorylation of Vav or Vav-2 was required for their GEF activity (9, 10). GEF activity of Dbl for Rho and Cdc42 was enhanced by tyrosine phosphorylation by ACK-1 (11). It was also demonstrated that several tyrosine kinase inhibitors blocked Gα12- or Gα13-mediated Rho activation in cells (12, 13). In addition, the involvement of Tec family tyrosine kinases in G12/13-mediated signaling pathway was demonstrated in cell-based assays as well as in *in vitro* experiments (14, 15). Tec kinases form a family of nonreceptor tyrosine kinases that share pleckstrin homology and Tec homology (TH) domains at the N-terminal region (16). These kinases are activated by various stimuli, including ligands for G protein-coupled receptors (17). However, their regulatory functions in cells remain unclear.

In this study, we investigated the possibility that RhoGEF other than p115 might be responsible for mediating signals from Gα12 to Rho. We found that leukemia-associated RhoGEF (LARG) could transduce Gα12-mediated Rho activation when it was phosphorylated by Tec tyrosine kinase.

Methods

Construction of Plasmids. KIAA0382 was originally isolated as a partial cDNA lacking N-terminal PDZ and RGS domains (18). Full-length cDNA was obtained by 5′-RACE using KIAA0382 as a template and human brain cDNA library (CLONTECH). The full-length cDNA had an identical amino acid sequence with LARG. LARG (1–1543), ΔPDZ-LARG (307–1543), ΔN-LARG (617–1543), PDZ-RhoGEF, p115RhoGEF, Tec (1–629), and kinase domain-deleted Tec (Tec-KD) (1–358) were subcloned into pcDNA-myc vector with N-terminal myc-tag. cDNAs for Tec lacking TH domain (ΔTH-Tec) and the constitutively active form of Tec (mHTec), which has N-terminal myristoylation signal, were subcloned into pSRα mammalian expression vector (17, 19). cDNAs encoding the constitutively active Gα12 (Gα12Q229L) and Gα13 (Gα13Q226L) were subcloned into pCMV5 vector. SRE.L-luciferase reporter plasmid and an expression construct for GST-fused RhoA binding domain of Rhotekin (GST-RBD) were kindly provided by P. C. Sternweis (University of Texas Southwestern Medical Center) and G. Bokoch (The Scripps Research Institute, La Jolla, CA), respectively.

SRE-Luciferase Assay. HeLa cells (6×10^4 cells per well) were plated onto 24-well plates 1 day before transfection. Cells were cotransfected with SRE.L-luciferase reporter plasmid (0.1 μg), pCMV-βgal (0.1 μg), and the indicated cDNAs. The cells were cultured in the presence of 10% FCS for 5 h and then serum-starved for 24 h. Luciferase activities in cell extracts were measured according to the manufacturer's instruction (Promega). Total amounts of transfected DNA were kept constant among wells by supplementing the empty vector DNA. β-Galactosidase activities of cell lysates were used to normalize for the transfection efficiency.

Expression and Purification of Proteins. The constructs of LARG were subcloned into the pFastBacHT transfer vector with a

This paper was submitted directly (Track II) to the PNAS office.

Abbreviations: GEF, guanine nucleotide exchange factor; LARG, leukemia-associated RhoGEF; TH, Tec homology.

‡To whom correspondence should be addressed. E-mail: tkozas@uic.edu.

six-histidine tag at the N terminus (Life Technologies, Grand Island, NY), and their recombinant baculoviruses were generated. Sf9 cells (1.8×10^6 cells per ml) were infected with corresponding recombinant baculovirus and harvested after 48 h. Cells were resuspended in lysis buffer (20 mM Hepes, pH 8.0/50 mM NaCl/0.1 mM EDTA/10 mM 2-mercaptoethanol and protease inhibitors) and lysed by nitrogen cavitation. The lysates were centrifuged at 100,000 × *g* and 4°C for 30 min. The supernatants were loaded onto Ni-NTA column equilibrated with buffer A (20 mM Hepes, pH 8.0/100 mM NaCl/10 mM 2-mercaptoethanol). The column was washed with 10 column volumes of buffer B (buffer A containing 400 mM NaCl and 10 mM imidazole). Recombinant LARG was eluted by 10 column volumes of buffer C (buffer A containing 150 mM imidazole). The elution fractions were concentrated and the buffer was exchanged with buffer D (buffer A containing 10% glycerol).

p115RhoGEF and RhoA were prepared as described (6, 7). Gα12 and Gα13 were purified using the Sf9-baculovirus expression system as described (20), with the following modification for Gα13 purification. Instead of 1% octylglucoside, 0.2% *n*-dodecyl-β-D-maltoside and 10% glycerol were included in the elution buffer of Gα13 from Ni-NTA column.

RhoGEF Assay. RhoA loaded with [^{3}H]GDP (100 nM, 2,000 cpm/pmol) was incubated with the indicated proteins at 20°C in GEF assay buffer (50 mM Tris·HCl, pH 7.5/50 mM NaCl/1 mM EDTA/1 mM DTT/10 mM $MgCl_2$/5 μM GTPγS/0.1% $C_{12}E_{10}$) in a final volume of 20 μl. G protein α subunits were preincubated in the presence of AMF (30 μM $AlCl_3$/5 mM $MgCl_2$/10 mM NaF) and added to the GEF reaction mixture. The reactions were stopped by the addition of 2 ml of washing buffer (20 mM Tris·HCl, pH 7.5/40 mM $MgSO_4$/100 mM NaCl), followed by filtration through BA-85 filters (Schleicher & Schuell). The amount of [^{3}H]GDP that remained on the filter was determined by a liquid scintillation counter.

To prepare Tec for GEF assays, COS1 cells were transfected with myc-tagged Tec. After 24 h, cells were lysed in the lysis buffer (50 mM Tris·HCl/150 mM NaCl/1% Nonidet P-40/1 mM EDTA/1 mM DTT/10 mM β-glycerophosphate/10 mM Na_3VO_4 and protease inhibitors) and centrifuged at 200,000 × *g* for 20 min. The supernatants were incubated with anti-myc antibody 9E10 (Covance). Tec was immunoprecipitated using protein G-agarose (Santa Cruz Biotechnology) and resuspended in GEF buffer.

To prepare phosphorylated LARG, Tec immunoprecipitated from COS1 cells was mixed with LARG and incubated at 20°C for 40 min in GEF buffer with 100 μM ATP. Then, [^{3}H]GDP-loaded RhoA (100 nM) and AlF_4^--activated Gα were added to the GEF reaction mixture. The mixture was further incubated at 20°C for the indicated time. The dissociation of GDP from RhoA was measured as described above.

To measure RhoGEF activity in cells, endogenous GTP-bound RhoA in cell lysate were detected by their association with GST–RBD as described by Ren and Schwartz (21).

Phosphorylation Assay. Tec or Tec-KD was overexpressed in COS1 cells, prepared as described above, and was resuspended in the kinase buffer (20 mM Tris·HCl, pH 7.4/50 mM NaCl/10 mM $MgCl_2$/2 mM $MnSO_4$/100 μM ATP). RhoGEF with or without Gα12/13 was incubated with Tec in the kinase buffer at 30°C for 20 min. The reactions were terminated by adding SDS/PAGE sample buffer, and the samples were separated by SDS/PAGE, followed by immunoblotting using anti-Tec antibody (17) or antiphosphotyrosine antibody PY20 (Zymed).

For the assessment of phosphorylation *in vivo*, HEK293 cells were cotransfected with myc-tagged ΔPDZ-LARG, ΔN-LARG, or p115 and the constitutively active Tec (mHTec). After 24 h, cells were lysed and LARG was immunoprecipitated by anti-myc antibody. The immunoprecipitates were subjected to SDS/PAGE and analyzed by immunoblotting with PY20 antibody.

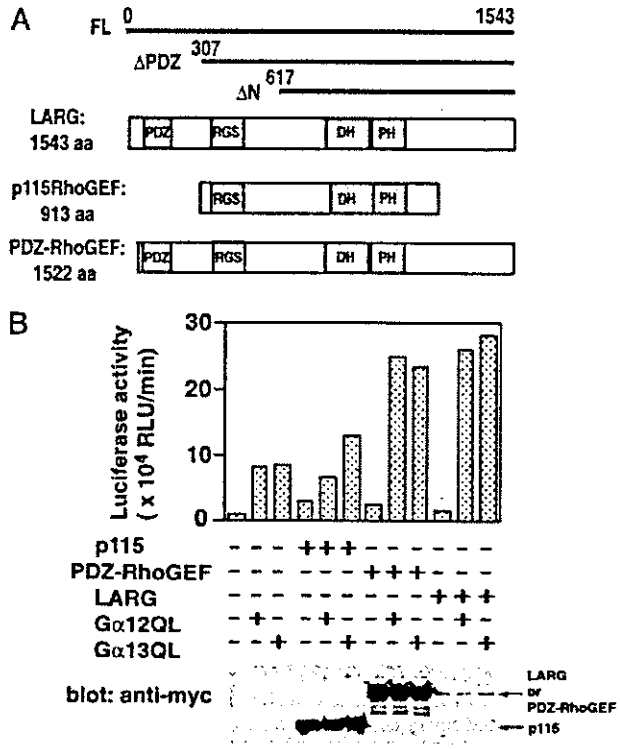

Fig. 1. Involvement of LARG and PDZ-RhoGEF in Gα12/13-mediated SRF activation. (*A*) Domain structure of RhoGEFs. Domains of p115RhoGEF, LARG, and PDZ-RhoGEF are schematically represented. PDZ, PDZ domain; RGS, RGS domain; DH, Dbl homology domain; PH, pleckstrin homology domain. The constructs of LARG that were used in this study are shown at the top. (*B*) SRF activation by Gα12/13-RhoGEF. HeLa cells were cotransfected with 0.1 μg of SRE.L-luciferase reporter plasmid and the indicated constructs: 0.01 μg of Gα12QL, 0.01 μg of Gα13QL, 0.1 μg of PDZ-RhoGEF, 0.1 μg of LARG, or 0.02 μg of p115RhoGEF. SRF activities of cell lysates were measured 24 h after transfection as described in *Methods*. The expression of RhoGEFs in lysates was detected by immunoblotting using anti-myc antibody as shown (*Lower*).

Miscellaneous Procedures. Immunoblotting was performed using the chemiluminescent detection system (Pierce). GTPase assays for Gα subunits were performed as described (6).

Results

In addition to p115RhoGEF, two mammalian RhoGEFs, PDZ-RhoGEF (KIAA0380) and LARG, were identified to have an RGS domain in their N-terminal region (refs. 18 and 22; Fig. 1*A*). It was shown that PDZ-RhoGEF and LARG interacted with constitutively active mutants of Gα12 and Gα13 through their RGS domains (23, 24). However, the biochemical mechanism to regulate the RhoGEF activity of PDZ-RhoGEF or LARG by Gα12/13 has not been elucidated. To examine whether PDZ-RhoGEF or LARG can mediate the signal from Gα12 or Gα13 to Rho activation, we first performed SRE-luciferase reporter assays. It has already been shown that Gα12/13-mediated Rho activation could be monitored in cells by SRF activation (25). As shown in Fig. 1*B*, overexpression of a constitutively active mutant of Gα12 (Gα12Q229L) or Gα13 (Gα13Q226L) modestly stimulated SRF activity, whereas coexpression of these mutants with LARG or PDZ-RhoGEF synergistically potentiated SRF activation. In particular, SRF activation by PDZ-RhoGEF or LARG